# CHAPTER 11

# FREQUENCY INDEPENDENT ANTENNAS AND ANTENNA MINIATURIZATION

## 11.1 INTRODUCTION

The numerous applications of electromagnetics to the advances of technology have necessitated the exploration and utilization of most of the electromagnetic spectrum. In addition, the advent of broadband systems have demanded the design of broadband radiators. The use of simple, small, lightweight, and economical antennas, designed to operate over the entire frequency band of a given system, would be most desirable. Although in practice all the desired features and benefits cannot usually be derived from a single radiator, most can effectively be accommodated. Previous to the 1950s, antennas with broadband pattern and impedance characteristics had bandwidths not greater than 2:1. In the 1950s, a breakthrough in antenna evolution was made which extended the bandwidth to as great as 40:1 or more. The antennas introduced by the breakthrough were referred to as *frequency independent*, and they had geometries that were specified by angles. These antennas are primarily used in the 10–10,000 MHz region in a variety of practical applications such as TV, point-to-point communication, feeds for reflectors and lenses, and so forth.

In antenna scale modeling, characteristics such as impedance, pattern, polarization, and so forth, are invariant to a change of the physical size if a similar change is also made in the operating frequency or wavelength. For example, if *all* the physical dimensions are *reduced* by a factor of two, the performance of the antenna will remain unchanged if the operating frequency is *increased* by a factor of two. In other words, the performance is invariant if the electrical dimensions remain unchanged. This is the principle on which antenna scale model measurements are made. For a complete and thorough discussion of scaling, the reader is referred to Section 16.10 entitled "Scale Model Measurements."

The scaling characteristics of antenna model measurements also indicate that if the shape of the antenna were completely specified by angles, its performance would have to be independent of frequency [1]. The infinite biconical dipole of Figure 9.1 is one such structure. To make infinite structures more practical, the designs usually

require that the current on the structure decrease with distance away from the input terminals. After a certain point the current is negligible, and the structure beyond that point to infinity can be truncated and removed. Practically then the truncated antenna has a lower cutoff frequency above which its radiation characteristics are the same as those of the infinite structure. The lower cutoff frequency is that for which the current at the point of truncation becomes negligible. The upper cutoff is limited to frequencies for which the dimensions of the feed transmission line cease to look like a "point" (usually about $\lambda_2/8$ where $\lambda_2$ is the wavelength at the highest desirable frequency). Practical bandwidths are on the order of about 40:1. Even higher ratios (i.e., 1,000:1) can be achieved in antenna design but they are not necessary, since they would far exceed the bandwidths of receivers and transmitters.

Even though the shape of the biconical antenna can be completely specified by angles, the current on its structure does not diminish with distance away from the input terminals, and its pattern does not have a limiting form with frequency. This can be seen by examining the current distribution as given by (9-11). It is evident that there are phase but no amplitude variations with the radial distance $r$. Thus the biconical structure cannot be truncated to form a frequency independent antenna. In practice, however, antenna shapes exist which satisfy the general shape equation, as proposed by Rumsey [1], to have frequency independent characteristics in pattern, impedance, polarization, and so forth, and with current distribution which diminishes rapidly.

Rumsey's general equation will first be developed, and it will be used as the unifying concept to link the major forms of frequency independent antennas. Classical shapes of such antennas include the equiangular geometries of planar and conical spiral structures investigated thoroughly by Dyson [2], [3], and the logarithmically periodic structures proposed and developed by DuHamel and Isbell [4], [5].

Fundamental limitations in electrically small antennas will be discussed in Section 11.5. These will be derived using spherical mode theory, with the antenna enclosed in a virtual sphere. Minimum $Q$ curves, which place limits on the achievable bandwidth, will be included.

## 11.2 THEORY

The analytical treatment of frequency independent antennas presented here parallels that introduced by Rumsey [1] and simplified by Elliott [6] for three-dimensional configurations.

We begin by assuming that an antenna, whose geometry is best described by the spherical coordinates $(r, \theta, \phi)$, has both terminals infinitely close to the origin and each is symmetrically disposed along the $\theta = 0, \pi$-axes. It is assumed that the antenna is perfectly conducting, it is surrounded by an infinite homogeneous and isotropic medium, and its surface or an edge on its surface is described by a curve

$$r = F(\theta, \phi) \tag{11-1}$$

where $r$ represents the distance along the surface or edge. If the antenna is to be scaled to a frequency that is $K$ times lower than the original frequency, the antenna's physical surface must be made $K$ times greater to maintain the same electrical dimensions. Thus the new surface is described by

$$r' = KF(\theta, \phi) \tag{11-2}$$

The new and old surfaces are identical; that is, not only are they similar but they are also congruent (if both surfaces are infinite). Congruence can be established only by

rotation in $\phi$. Translation is not allowed because the terminals of both surfaces are at the origin. Rotation in $\theta$ is prohibited because both terminals are symmetrically disposed along the $\theta = 0, \pi$-axes.

For the second antenna to achieve congruence with the first, it must be rotated by an angle $C$ so that

$$KF(\theta, \phi) = F(\theta, \phi + C) \tag{11-3}$$

The angle of rotation $C$ depends on $K$ but neither depends on $\theta$ or $\phi$. Physical congruence implies that the original antenna electrically would behave the same at both frequencies. However the radiation pattern will be rotated azimuthally through an angle $C$. For unrestricted values of $K$ ($0 \leq K \leq \infty$), the pattern will rotate by $C$ in $\phi$ with frequency, because $C$ depends on $K$, but its shape will be unaltered. Thus the impedance and pattern will be frequency independent.

To obtain the functional representation of $F(\theta, \phi)$, both sides of (11-3) are differentiated with respect to $C$ to yield

$$\begin{aligned} \frac{d}{dC}[KF(\theta, \phi)] &= \frac{dK}{dC}F(\theta, \phi) = \frac{\partial}{\partial C}[F(\theta, \phi + C)] \\ &= \frac{\partial}{\partial(\phi + C)}[F(\theta, \phi + C)] \end{aligned} \tag{11-4}$$

and with respect to $\phi$ to give

$$\begin{aligned} \frac{\partial}{\partial \phi}[KF(\theta, \phi)] &= K\frac{\partial F(\theta, \phi)}{\partial \phi} = \frac{\partial}{\partial \phi}[F(\theta, \phi + C)] \\ &= \frac{\partial}{\partial(\phi + C)}[F(\theta, \phi + C)] \end{aligned} \tag{11-5}$$

Equating (11-5) to (11-4) yields

$$\frac{dK}{dC}F(\theta, \phi) = K\frac{\partial F(\theta, \phi)}{\partial \phi} \tag{11-6}$$

Using (11-1) we can write (11-6) as

$$\frac{1}{K}\frac{dK}{dC} = \frac{1}{r}\frac{\partial r}{\partial \phi} \tag{11-7}$$

Since the left side of (11-7) is independent of $\theta$ and $\phi$, a general solution for the surface $r = F(\theta, \phi)$ of the antenna is

$$r = F(\theta, \phi) = e^{a\phi}f(\theta) \tag{11-8}$$

where

$$a = \frac{1}{K}\frac{dK}{dC} \tag{11-8a}$$

and $f(\theta)$ is a completely arbitrary function.

Thus for any antenna to have frequency independent characteristics, its surface must be described by (11-8). This can be accomplished by specifying the function $f(\theta)$ or its derivatives. Subsequently, interesting, practical, and extremely useful antenna configurations will be introduced whose surfaces are described by (11-8).

## 11.3 EQUIANGULAR SPIRAL ANTENNAS

The equiangular spiral is one geometrical configuration whose surface can be described by angles. It thus fulfills all the requirements for shapes that can be used to design frequency independent antennas. Since a curve along its surface extends to infinity, it is necessary to designate the length of the arm to specify a finite size antenna. The lowest frequency of operation occurs when the total arm length is comparable to the wavelength [2]. For all frequencies above this, the pattern and impedance characteristics are frequency independent.

### 11.3.1 Planar Spiral

The shape of an equiangular plane spiral curve can be derived by letting the derivative of $f(\theta)$ in (11-8) be

$$\frac{df}{d\theta} = f'(\theta) = A\delta\left(\frac{\pi}{2} - \theta\right) \tag{11-9}$$

where $A$ is a constant and $\delta$ is the Dirac delta function. Using (11-9) reduces (11-8) to

$$r|_{\theta=\pi/2} = \rho = \begin{cases} Ae^{a\phi} = \rho_0 e^{a(\phi-\phi_0)} & \theta = \pi/2 \\ 0 & \text{elsewhere} \end{cases} \tag{11-10}$$

where

$$A = \rho_0 e^{-a\phi_0} \tag{11-10a}$$

In wavelengths, (11-10) can be written as

$$\rho_\lambda = \frac{\rho}{\lambda} = \frac{A}{\lambda}e^{a\phi} = Ae^{a|\phi - \ln(\lambda)/a|} = Ae^{a(\phi-\phi_1)} \tag{11-11}$$

where

$$\phi_1 = \frac{1}{a}\ln(\lambda) \tag{11-11a}$$

Another form of (11-10) is

$$\phi = \frac{1}{a}\ln\left(\frac{\rho}{A}\right) = \tan\psi \ln\left(\frac{\rho}{A}\right) = \tan\psi(\ln\rho - \ln A) \tag{11-12}$$

where $1/a$ is the rate of expansion of the spiral and $\psi$ is the angle between the radial distance $\rho$ and the tangent to the spiral, as shown in Figure 11.1(a).

It is evident from (11-11) that changing the wavelength is equivalent to varying $\phi_0$ which results in nothing more than a pure rotation of the infinite structure pattern. Within limitations imposed by the arm length, similar characteristics have been observed for finite structures. The same result can be concluded by examining (11-12). Increasing the logarithm of the frequency ($\ln f$) by $C_0$ is equivalent to rotating the structure by $C_0 \tan\psi$. As a result, the pattern is merely rotated but otherwise unaltered. Thus we have frequency independent antennas.

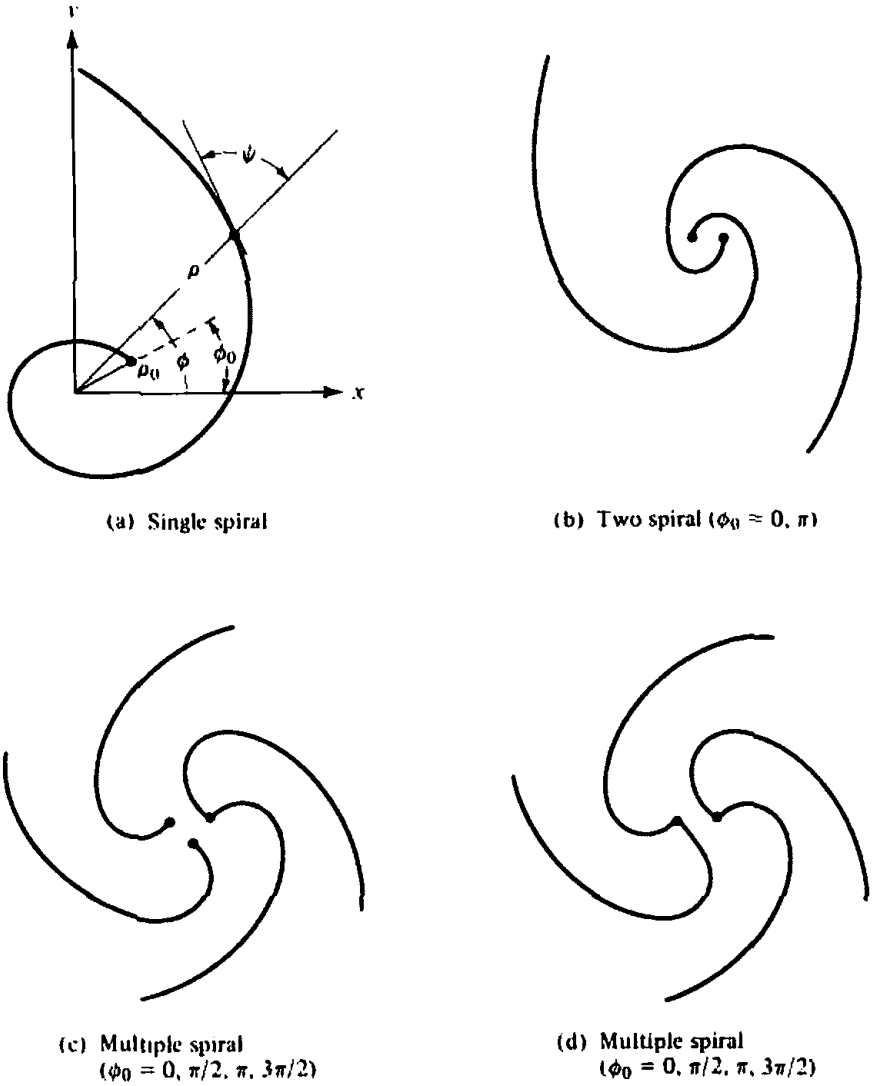


(a) Single spiral

(b) Two spiral ($\phi_0 = 0, \pi$)

(c) Multiple spiral ($\phi_0 = 0, \pi/2, \pi, 3\pi/2$)

(d) Multiple spiral ($\phi_0 = 0, \pi/2, \pi, 3\pi/2$)

**Figure 11.1** Spiral wire antennas.

The total length $L$ of the spiral can be calculated by

$$L = \int_{\rho_0}^{\rho_1} \left[ \rho^2 \left( \frac{d\phi}{d\rho} \right)^2 + 1 \right]^{1/2} d\rho \tag{11-13}$$

which reduces, using (11-10), to

$$\boxed{L = (\rho_1 - \rho_0)\sqrt{1 + \frac{1}{a^2}}} \tag{11-14}$$

where $\rho_0$ and $\rho_1$ represent the inner and outer radii of the spiral.

Various geometrical arrangements of the spiral have been used to form different antenna systems. If $\phi_0$ in (11-10) is 0 and $\pi$, the spiral wire antenna takes the form of Figure 11.1(b). The arrangements of Figures 11.1(c) and 11.1(d) are each obtained when $\phi_0 = 0, \pi/2, \pi$, and $3\pi/2$. Numerous other combinations are possible.

An equiangular metallic solid surface, designated as $P$, can be created by defining the curves of its edges, using (11-10), as

$$\rho_2 = \rho_2' e^{a\phi} \tag{11-15a}$$

$$\rho_3 = \rho_3' e^{a\phi} = \rho_2' e^{a(\phi - \delta)} \tag{11-15b}$$

where

$$\rho_3' = \rho_2' e^{-a\delta} \tag{11-15c}$$

such that

$$K = \frac{\rho_3}{\rho_2} = e^{-a\delta} < 1 \tag{11-16}$$

The two curves, which specify the edges of the conducting surface, are of identical relative shape with one magnified relative to the other or rotated by an angle $\delta$ with respect to the other. The magnification or rotation allows the arm of conductor $P$ to have a finite width, as shown in Figure 11.2(a).

The metallic arm of a second conductor, designated as $Q$, can be defined by

$$\rho_4 = \rho_4' e^{a\phi} = \rho_2' e^{a(\phi - \pi)} \tag{11-17}$$

where

$$\rho_4' = \rho_2' e^{-a\pi} \tag{11-17a}$$

$$\rho_5 = \rho_5' e^{a\phi} = \rho_4' e^{a(\phi - \delta)} = \rho_2' e^{a(\phi - \pi - \delta)} \tag{11-18}$$

where

$$\rho_5' = \rho_4' e^{-a\delta} = \rho_2' e^{-a(\pi + \delta)} \tag{11-18a}$$

The system composed of the two conducting arms, $P$ and $Q$, constitutes a balanced system, and it is shown in Figure 11.2(a). The finite size of the structure is specified by the fixed spiraling length $L_0$ along the centerline of the arm. The entire structure can be completely specified by the rotation angle $\delta$, the arm length $L_0$, the rate of spiral $1/a$, and the terminal size $\rho_2'$. However, it has been found that most characteristics can be described adequately by only three; that is, $L_0$, $\rho_2'$, and $K = e^{-a\delta}$ as given by (11-16). In addition each arm is usually tapered at its end, shown by dashed lines in Figure 11.2(a), to provide a better matching termination.

The previous analytical formulations can be used to describe two different antennas. One antenna would consist of two metallic arms suspended in free-space, as shown in Figure 11.2(a), and the other of a spiraling slot on a large conducting plane, as shown in Figure 11.2(b). The second is also usually tapered to provide better matching termination. The slot antenna is the most practical, because it can be conveniently fed by a balanced coaxial arrangement [2] to maintain its overall balancing. The antenna in Figure 11.2(a) with $\delta = \pi/2$ is self-complementary, as defined by Babinet's principle [7], and its input impedance for an infinite structure should be $Z_s = Z_c = 188.5 = 60\pi$ ohms (for discussion of Babinet's Principle see Section 12.8). Experimentally, measured mean input impedances were found to be only about 164 ohms. The difference between theory and experiment is attributed to the finite arm length, finite thickness of the plate, and nonideal feeding conditions.

Spiral slot antennas, with good radiation characteristics, can be built with one-half to three turns. The most optimum design seems to be that with 1.25 to 1.5 turns with an overall length equal to or greater than one wavelength. The rate of expansion should not exceed about 10 per turn. The patterns are bidirectional, single-lobed, broadside (maximum normal to the plane), and must vanish along the directions occupied by the infinite structure. The wave is circularly polarized near the axis of the main lobe over the usable part of the bandwidth. For a fixed cut, the beamwidth will vary with frequency since the pattern rotates. Typical variations are on the order of 10°. In general, however, slot antennas with more broad arms and/or more tightly

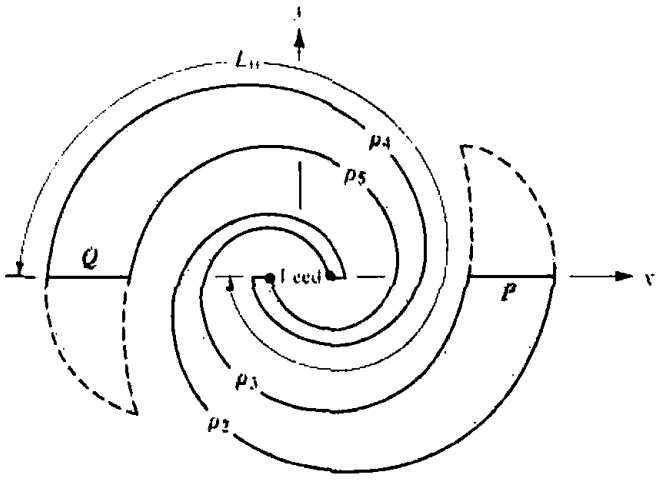


(a) Spiral plate

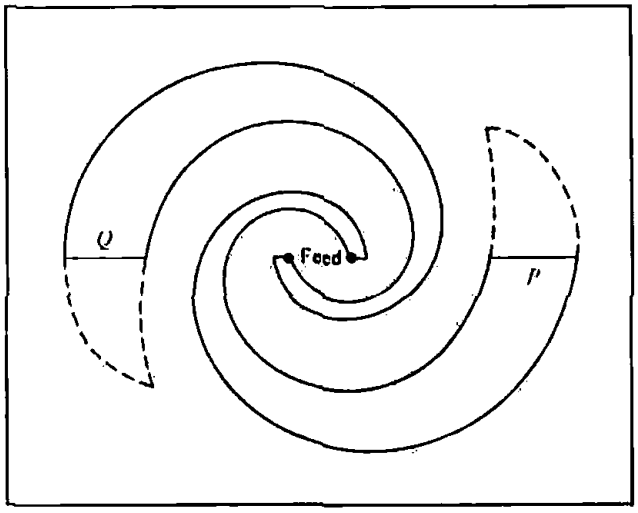


(b) Spiral slot

**Figure 11.2** Spiral plate and slot antennas.

wound spirals exhibit smoother and more uniform patterns with smaller variations in beamwidth with frequency. For symmetrical structures, the pattern is also symmetrical with no tilt to the lobe structure.

To maintain the symmetrical characteristics, the antenna must be fed by an electrically and geometrically balanced line. One method that achieves geometrical balancing requires that the coax is embedded into one of the arms of the spiral. To maintain symmetry, a dummy cable is usually placed into the other arm. No appreciable currents flow on the feed cables because of the rapid attenuation of the fields along the spiral. If the feed line is electrically unbalanced, a balun must be used. This limits the bandwidth of the system.

The polarization of the radiated wave is controlled by the length of the arms. For very low frequencies, such that the total arm length is small compared to the wavelength, the radiated field is linearly polarized. As the frequency increases, the wave becomes elliptically polarized and eventually achieves circular polarization. Since the pattern is essentially unaltered through this frequency range, the polarization change with frequency can be used as a convenient criterion to select the lower cutoff

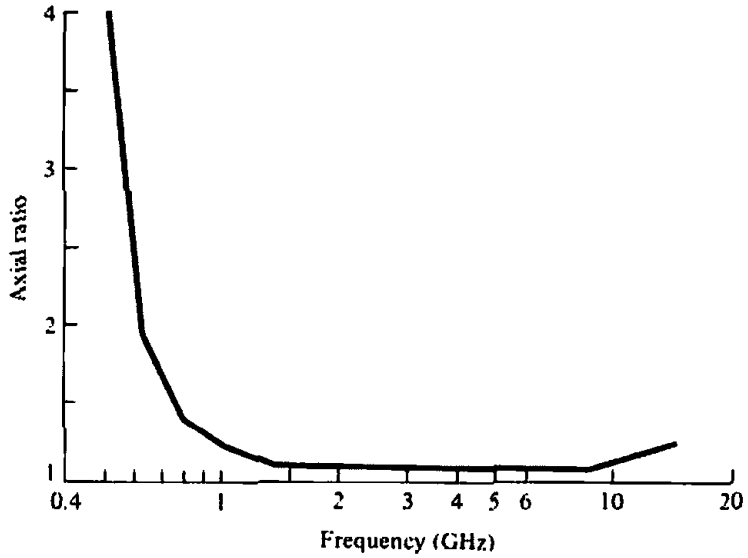


**Figure 11.3** On-axis polarization as a function of frequency for one-turn spiral slot. (SOURCE: J. D. Dyson, "The Equiangular Spiral Antenna," *IRE Trans. Antennas Propagat.*, Vol. AP-7, pp. 181–187, April 1959. © (1959) IEEE)

frequency of the usable bandwidth. In many practical cases, this is chosen to be the point where the axial ratio is equal or less than 2 to 1, and it occurs typically when the overall armlength is about one wavelength. A typical variation in axial ratio of the on-axis field as a function of frequency for a one-turn slot antenna is shown in Figure 11.3. The off-axis radiated field has nearly circular polarization over a smaller part of the bandwidth. In addition to the limitation imposed on the bandwidth by the overall length of the arms, another critical factor that can extend or reduce the bandwidth is the construction precision of the feed.

The input impedance of a balanced equiangular slot antenna converges rapidly as the frequency is increased, and it remains reasonably constant for frequencies for which the arm length is greater than about one wavelength. Measured values for a 700–2,500 MHz antenna [2] were about 75–100 ohms with VSWR's of less than 2 to 1 for 50-ohm lines.

For slot antennas radiating in free-space, without dielectric material or cavity backing, typical measured efficiencies are about 98% for arm lengths equal to or greater than one wavelength. Rapid decreases are observed for shorter arms.

### 11.3.2 Conical Spiral

The shape of a nonplanar spiral can be described by defining the derivative of $f(\theta)$ to be

$$\frac{df}{d\theta} = f'(\theta) = A\delta(\beta - \theta) \tag{11-19}$$

in which $\beta$ is allowed to take any value in the range $0 \leq \beta \leq \pi$. For a given value of $\beta$, (11-19) in conjunction with (11-8) describes a spiral wrapped on a conical surface. The edges of one conical spiral surface are defined by

$$r_2 = r_2' e^{(a \sin \theta_0)\phi} = r_2' e^{b\phi} \tag{11-20a}$$

$$r_3 = r_3' e^{a \sin \theta_0 \phi} = r_2' e^{a \sin \theta_0 (\phi - \delta)} \tag{11-20b}$$

where

$$r_3' = r_2' e^{-(a \sin \theta_0)\delta} \tag{11-20c}$$

and $\theta_0$ is half of the total included cone angle. Larger values of $\theta_0$ in $0 \leq \theta \leq \pi/2$ represent less tightly wound spirals. These equations correspond to (11-15a)–(11-15c) for the planar surface. The second arm of a balanced system can be defined by shifting each of (11-20a)–(11-20c) by 180°, as was done for the planar surface by (11-17)–(11-18a). A conical spiral metal strip antenna of elliptical polarization is shown in Figure 11.4 [8].

The conducting conical spiral surface can be constructed conveniently by forming, using printed circuit techniques, the conical arms on the dielectric cone which is also used as a support. The feed cable can be bonded to the metal arms which are wrapped around the cone. Symmetry can be preserved by observing the same precautions, like the use of a dummy cable, as was done for the planar surface.

A distinct difference between the planar and conical spirals is that the latter provides unidirectional radiation (single lobe) toward the apex of the cone with the maximum along the axis. Circular polarization and relatively constant impedances are preserved over large bandwidths. Smoother patterns have been observed for unidirectional designs. Conical spirals can be used in conjunction with a ground plane, with a reduction in bandwidth when they are flush-mounted on the plane.

**Figure 11.4** Conical spiral metal strip antenna. (SOURCE: *Antennas, Antenna Masts and Mounting Adaptors*, American Electronic Laboratories, Inc., Lansdale, Pa., Catalog 7.5M-7-79. Courtesy of American Electronic Laboratories, Inc., Montgomeryville, PA 18936 USA)

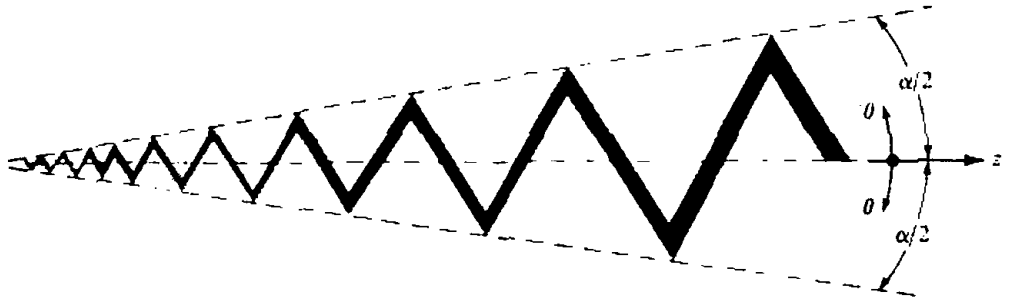


(a) Metal strip log-periodic configuration

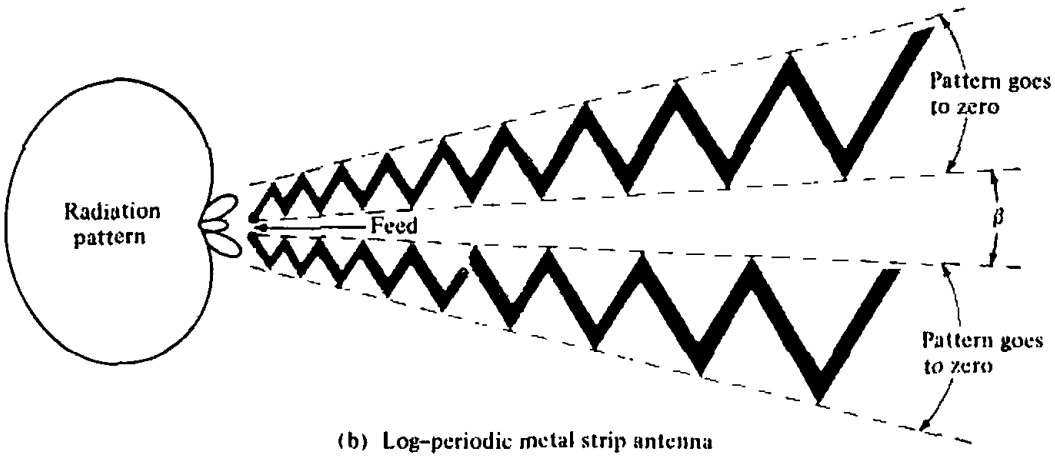


(b) Log-periodic metal strip antenna

**Figure 11.5** Typical metal strip log-periodic configuration and antenna structure.

## 11.4 LOG-PERIODIC ANTENNAS

Another type of an antenna configuration, which closely parallels the frequency independent concept, is the log-periodic structure introduced by DuHamel and Isbell [4]. Because the entire shape of it cannot be solely specified by angles, it is not truly frequency independent.

### 11.4.1 Planar and Wire Surfaces

A planar log-periodic structure is shown in Figure 11.5(a). It consists of a metal strip whose edges are specified by the angle $\alpha/2$. However, in order to specify the length from the origin to any point on the structure, a distance characteristic must be included.

In spherical coordinates $(r, \theta, \phi)$ the shape of the structure can be written as

$$\theta = \text{periodic function of } [b \ln(r)] \tag{11-21}$$

An example of it would be

$$\theta = \theta_0 \sin\left[b \ln\left(\frac{r}{r_0}\right)\right] \tag{11-22}$$

It is evident from (11-22) that the values of $\theta$ are repeated whenever the logarithm of the radial frequency $\ln(\omega) = \ln(2\pi f)$ differs by $2\pi/b$. The performance of the system is then periodic as a function of the logarithm of the frequency; thus the name *logarithmic-periodic or log-periodic.*

A typical log-periodic antenna configuration is shown in Figure 11.5(b). It consists of two coplanar arms of the Figure 11.5(a) geometry. The pattern is unidirectional

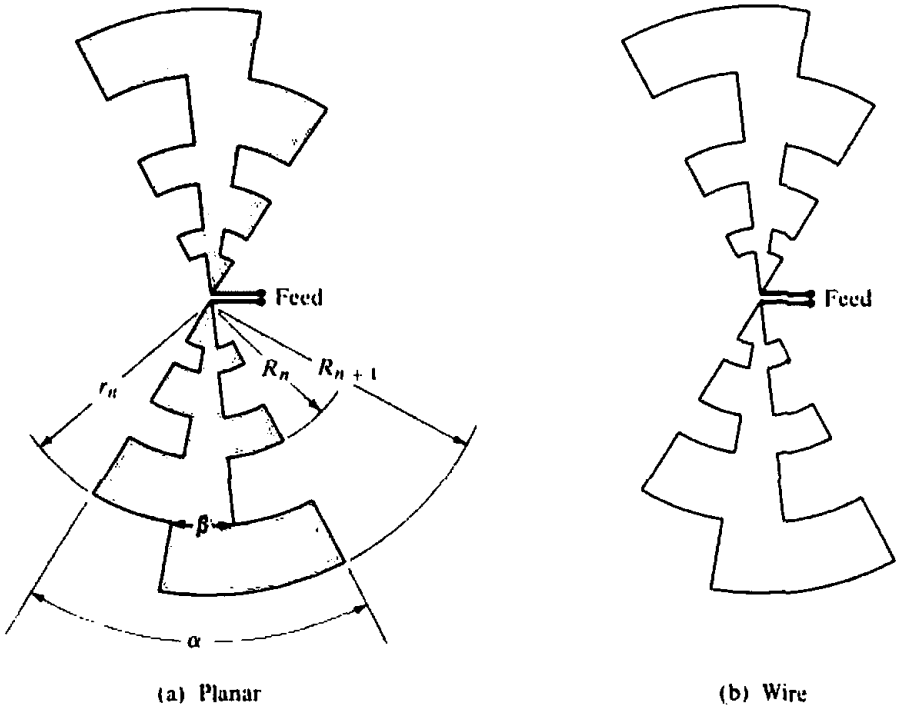


(a) Planar (b) Wire

**Figure 11.6** Planar and wire logarithmically periodic antennas.

toward the apex of the cone formed by the two arms, and it is linearly polarized. Although the patterns of this and other log-periodic structures are not completely frequency independent, the amplitude variations of certain designs are very slight. Thus practically they are frequency independent.

Log-periodic wire antennas were introduced by DuHamel [4]. While investigating the current distribution on log-periodic surface structures of the form shown in Figure 11.6(a), he discovered that the fields on the conductors attenuated very sharply with distance. This suggested that perhaps there was a strong current concentration at or near the edges of the conductors. Thus removing part of the inner surface to form a wire antenna as shown in Figure 11.6(b) should not seriously degrade the performance of the antenna. To verify this, a wire antenna, with geometrical shape identical to the pattern formed by the edges of the conducting surface, was built and it was investigated experimentally. As predicted, it was found that the performance of this antenna was almost identical to that of Figure 11.6(a); thus the discovery of a much simpler, lighter in weight, cheaper, and less wind resistant antenna. Nonplanar geometries in the form of a V, formed by bending one arm relative to the other, are also widely used.

If the wires or the edges of the plates are linear (instead of curved), the geometries of Figure 11.6 reduce, respectively, to the trapezoidal tooth log-periodic structures of Figure 11.7. These simplifications result in more convenient fabrication geometries with no loss in operational performance. There are numerous other bizarre but practical configurations of log-periodic structures, including log-periodic arrays.

If the geometries of Figure 11.6 use uniform periodic teeth, we define the geometric ratio of the log-periodic structure by

$$\tau = \frac{R_n}{R_{n+1}} \tag{11-23}$$

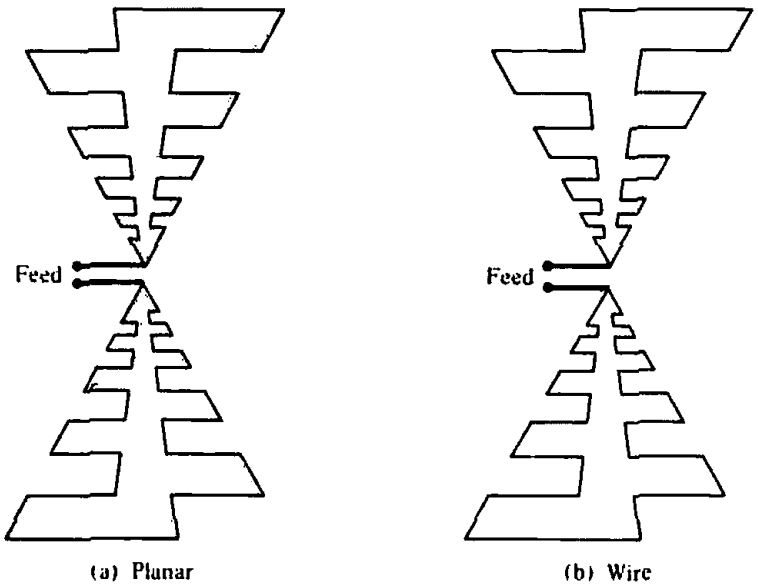


Figure 11.7 Planar and wire trapezoidal toothed log-periodic antennas.

and the width of the antenna slot by

$$\chi = \frac{r_n}{R_{n+1}} \tag{11-24}$$

The geometric ratio $\tau$ of (11-23) defines the period of operation. For example, if two frequencies $f_1$ and $f_2$ are one period apart, they are related to the geometric ratio $\tau$ by

$$\tau = \frac{f_1}{f_2}, \qquad f_2 > f_1 \tag{11-25}$$

Extensive studies on the performance of the antenna of Figure 11.6(b) as a function of $\alpha$, $\beta$, $\tau$, and $\chi$, have been performed [9]. In general, these structures performed almost as well as the planar and conical structures. The only major difference is that the log-periodic configurations are linearly polarized instead of circular.

A commercial lightweight, cavity-backed, linearly polarized, flush-mounted log-periodic slot antenna and its associated gain characteristics are shown in Figures 11.8(a) and (b) [8]. Typical electrical characteristics are: VSWR—2:1; $E$-plane beamwidth—70°; $H$-plane beamwidth—70°. The maximum diameter of the cavity is about 2.4 in. (6.1 cm), the depth is 1.75 in. (4.445 cm), and the weight is near 5 oz (0.14 kg).

### 11.4.2 Dipole Array

To the layman, the most recognized log-periodic antenna structure is the configuration introduced by Isbell [5] which is shown in Figure 11.9(a). It consists of a sequence of side-by-side parallel linear dipoles forming a coplanar array. Although this antenna has similar directivities as the Yagi-Uda array (7–12 dB), they are achievable and maintained over much wider bandwidths. There are, however, major differences between them.

While the geometrical dimensions of the Yagi-Uda array elements do not follow any set pattern, the lengths ($l_n$'s), spacings ($R_n$'s), diameters ($d_n$'s), and even gap

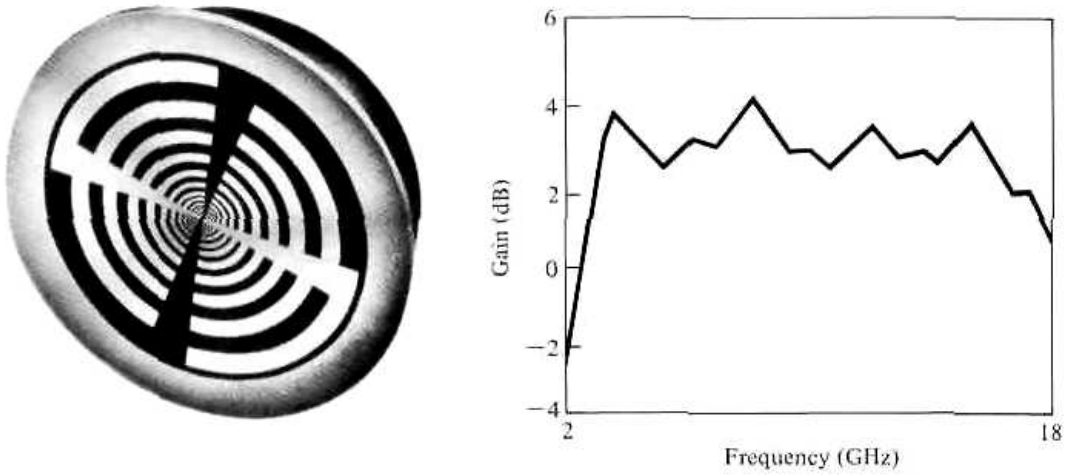


(a) Antenna (b) Gain characteristics

**Figure 11.8** Linearly polarized flush-mounted cavity-backed log-periodic slot antenna and typical gain characteristics. (SOURCE: *Antennas, Antenna Masts and Mounting Adaptors*, American Electronic Laboratories, Inc., Lansdale, Pa., Catalog 7.5M-7-79. Courtesy of American Electronic Laboratories, Inc., Montgomeryville, PA 18936 USA)

spacings at dipole centers ($s_n$'s) of the log-periodic array increase logarithmically as defined by the inverse of the geometric ratio $\tau$. That is,

$$\frac{1}{\tau} = \frac{l_2}{l_1} = \frac{l_{n+1}}{l_n} = \frac{R_2}{R_1} = \frac{R_{n+1}}{R_n} = \frac{d_2}{d_1} = \frac{d_{n+1}}{d_n} = \frac{s_2}{s_1} = \frac{s_{n+1}}{s_n} \tag{11-26}$$

Another parameter that is usually associated with a dipole array is the spacing factor $\sigma$ defined by

$$\sigma = \frac{R_{n+1} - R_n}{2l_{n+1}} \tag{11-26a}$$

Straight lines through the dipole ends meet to form an angle $2\alpha$ which is a characteristic of frequency independent structures.

Because it is usually very difficult to obtain wires or tubing of many different diameters and to maintain tolerances of very small gap spacings, constant dimensions in these can be used. These relatively minor factors will not sufficiently degrade the overall performance.

While only one element of the Yagi-Uda array is directly energized by the feed line, while the others operate in a parasitic mode, all the elements of the log-periodic array are connected. There are two basic methods, as shown in Figures 11.9(b) and 11.9(c), which could be used to connect and feed the elements of a log-periodic dipole array. In both cases the antenna is fed at the small end of the structure.

The currents in the elements of Figure 11.9(b) have the same phase relationship as the terminal phases. If in addition the elements are closely spaced, the phase progression of the currents is to the right. This produces an endfire beam in the direction of the longer elements and interference effects to the pattern result.

It was recognized that by mechanically crisscrossing or transposing the feed between adjacent elements, as shown in Figure 11.9(c), a 180° phase is added to the terminal of each element. Since the phase between the adjacent closely spaced short elements is almost in opposition, very little energy is radiated by them and their

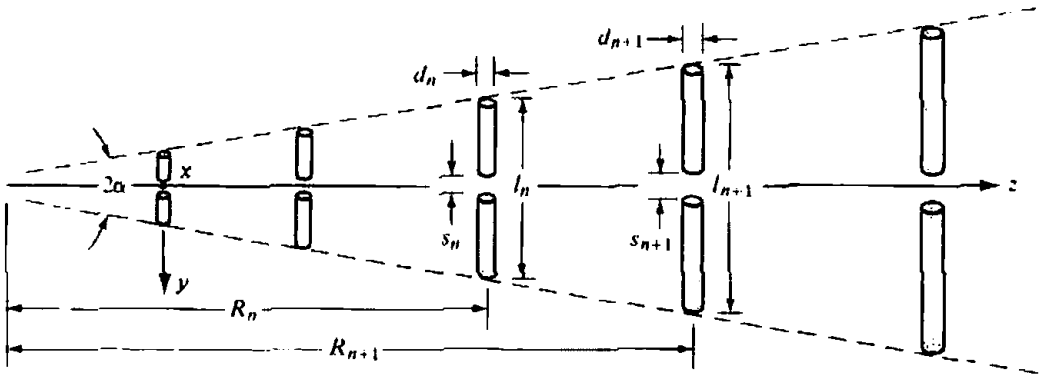


(a) Dipole array

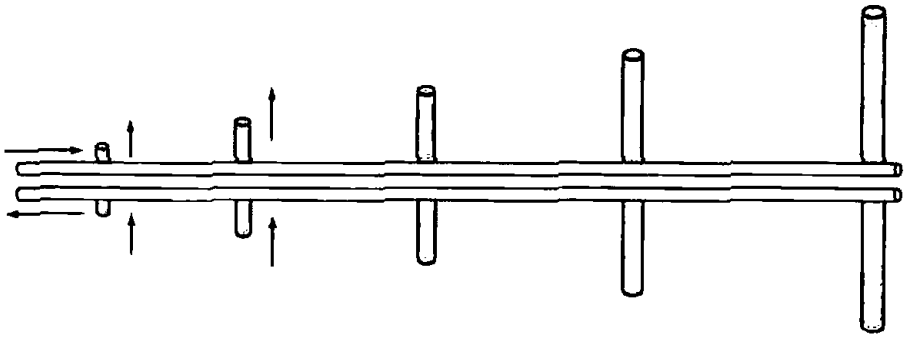

(b) Straight connection

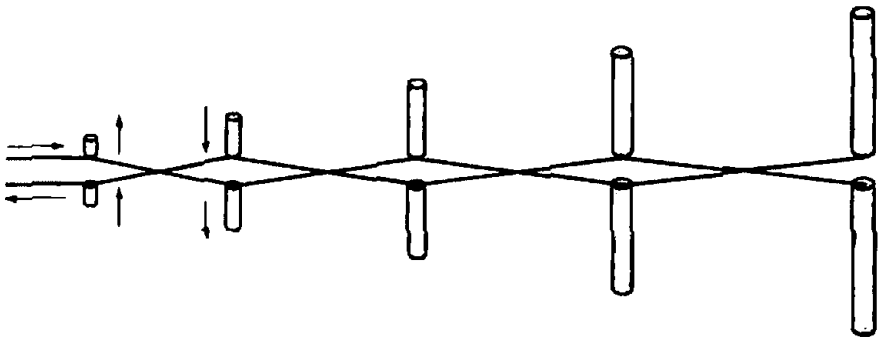

(c) Crisscross connection

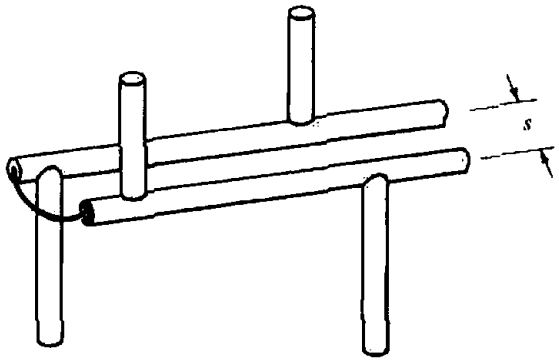


(d) Coaxial connection

**Figure 11.9** Log-periodic dipole array and associated connections.

interference effects are negligible. However, at the same time, the longer and larger spaced elements radiate. The mechanical phase reversal between these elements produces a phase progression so that the energy is beamed endfire in the direction of the shorter elements. The most active elements for this feed arrangement are those that are near resonant with a combined radiation pattern toward the vertex of the array.

The feed arrangement of Figure 11.9(c) is convenient provided the input feed line is a balanced line like the two-conductor transmission line. Using a coaxial cable as a feed line, a practical method to achieve the 180° phase reversal between adjacent elements is shown in Figure 11.9(d). This feed arrangement provides a built-in broadband balun resulting in a balanced overall system. The elements and the feeder line of this array are usually made of piping. The coaxial cable is brought to the feed through the hollow part of one of the feeder line pipes. While the outside conductor of the coax is connected to that conductor at the feed, its inner conductor is extended and it is connected to the other pipe of the feeder line.

If the geometrical pattern of the log-periodic array, as defined by (11-26), is to be maintained to achieve a truly log-periodic configuration, an infinite structure would result. However, to be useful as a practical broadband radiator, the structure is truncated at both ends. This limits the frequency of operation to a given bandwidth.

The cutoff frequencies of the truncated structure can be determined by the electrical lengths of the longest and shortest elements of the structure. The lower cutoff frequency occurs approximately when the longest element is $\lambda/2$; however, the high cutoff frequency occurs when the shortest element is nearly $\lambda/2$ only when the active region is very narrow. Usually it extends beyond that element. The active region of the log-periodic dipole array is near the elements whose lengths are nearly or slightly smaller than $\lambda/2$. The role of active elements is passed from the longer to the shorter elements as the frequency increases. Also the energy from the shorter active elements traveling toward the longer inactive elements decreases very rapidly so that a negligible amount is reflected from the truncated end. The movement of the active region of the antenna, and its associated phase center, is an undesirable characteristic in the design of feeds for reflector and lens antennas.

The decrease of energy toward the longer inactive elements is demonstrated in Figure 11.10(a). The curves represent typical computed and measured transmission line voltages (amplitude and phase) on a log-periodic dipole array [10] as a function of distance from its apex. These are feeder-line voltages at the base of the elements of an array with $\tau = 0.95$, $\sigma = 0.0564$, $N = 13$, and $l_n/d_n = 177$. The frequency of operation is such that element No. 10 is $\lambda/2$. The amplitude voltage is nearly constant from the first (the feed) to the eighth element while the corresponding phase is uniformly progressive. Very rapid decreases in amplitude and nonlinear phase variations are noted beyond the eighth element.

The region of constant voltage along the structure is referred to as the *transmission region*, because it resembles that of a matched transmission line. Along the structure, there is about 150° phase change for every $\lambda/4$ free-space length of transmission line. This indicates that the phase velocity of the wave traveling along the structure is $v_p = 0.6v_0$, where $v_0$ is the free-space velocity. The smaller velocity results from the shunt capacitive loading of the line by the smaller elements. The loading is almost constant per unit length because there are larger spacings between the longer elements.

The corresponding current distribution is shown in Figure 11.10(b). It is noted that the rapid decrease in voltage is associated with strong current excitation of elements 7–10 followed by a rapid decline. The region of high current excitation is

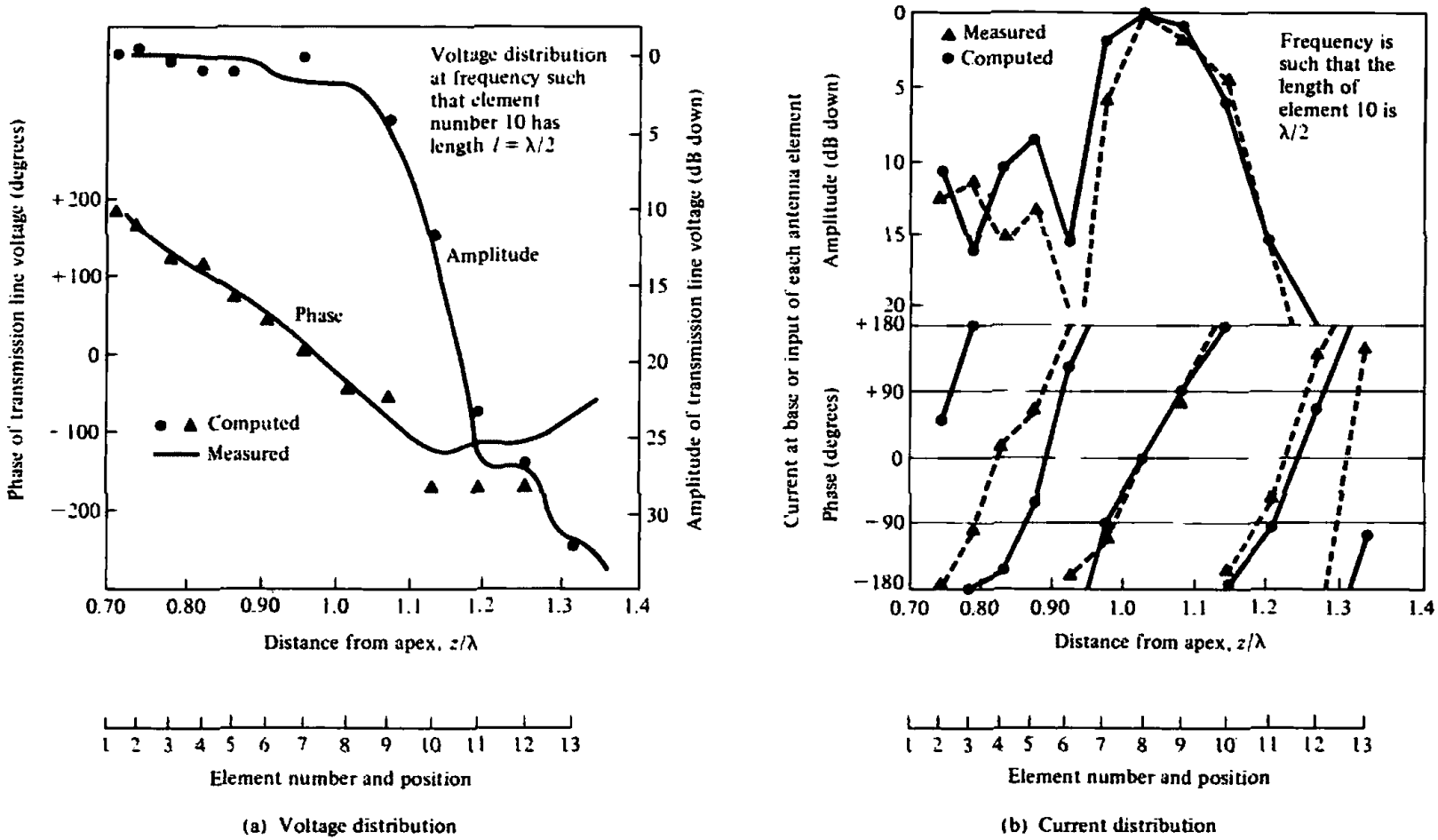


**Figure 11.10** Measured and computed voltage and current distributions on a log-periodic dipole array of 13 elements with frequency such that $l_{10} = \lambda/2$. (SOURCE: R. L. Carrel, "Analysis and Design of the Log-Periodic Dipole Antenna," Ph.D. Dissertation, Elec. Eng. Dept., University of Illinois, 1961, University Microfilms, Inc., Ann Arbor, Michigan)

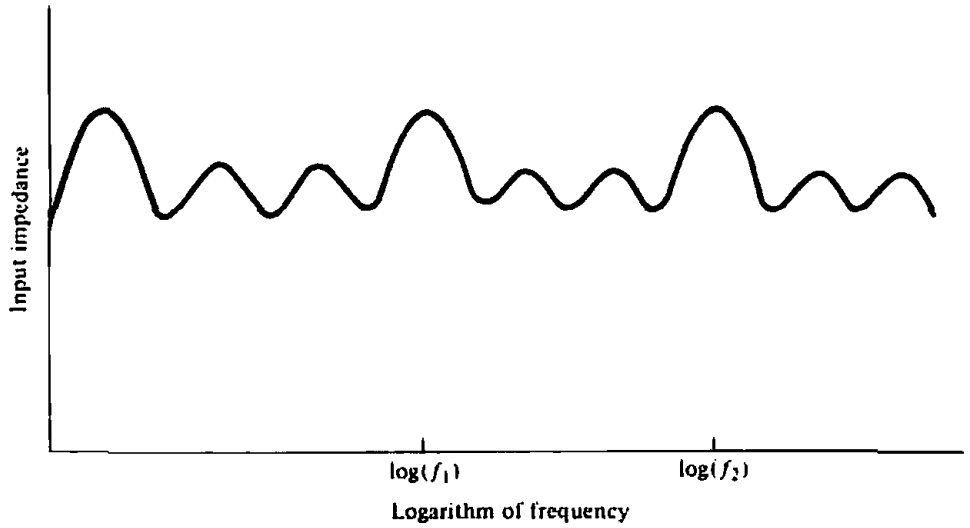


**Figure 11.11** Typical input impedance variation of a log-periodic antenna as a function of the logarithm of the frequency.

designated as the *active region*, and it encompasses 4 to 5 elements for this design. The voltage and current excitations of the longer elements (beyond the ninth) are relatively small, reassuring that the truncated larger end of the structure is not affecting the performance. The smaller elements, because of their length, are not excited effectively. As the frequency changes, the relative voltage and current patterns remain essentially the same, but they move toward the direction of the active region.

There is a linear increase in current phase, especially in the active region, from the shorter to the longer elements. This phase shift progression is opposite in direction to that of an unloaded line. It suggests that on the log-periodic antenna structure there is a wave that travels toward the feed forming a unidirectional endfire pattern toward the vertex.

The radiated wave of a single log-periodic dipole array is linearly polarized, and it has horizontal polarization when the plane of the antenna is parallel to the ground. Bidirectional patterns and circular polarization can be obtained by phasing multiple log-periodic dipole arrays. For these, the overall effective phase center can be maintained at the feed.

If the input impedance of a log-periodic antenna is plotted as a function of frequency, it will be repetitive. However, if it is plotted as a function of the *logarithm* of the frequency, it will be *periodic* (not necessarily sinusoidal) with each cycle being exactly identical to the preceding one. Hence the name *log-periodic*, because the variations are *periodic* with respect to the *logarithm* of the frequency. A typical variation of the impedance as a function of frequency is shown in Figure 11.11. Other parameters that undergo similar variations are the pattern, directivity, beamwidth, and side lobe level.

The periodicity of the structure does not ensure broadband operation. However, if the variations of the impedance, pattern, directivity, and so forth within one cycle are made sufficiently small and acceptable for the corresponding bandwidth of the cycle, broadband characteristics are ensured within acceptable limits of variation. The total bandwidth is determined by the number of repetitive cycles for the given truncated structure.

The relative frequency span $\Delta$ of each cycle is determined by the geometric ratio

TABLE 11.1 INPUT RESISTANCES ($R_{in}$ IN OHMS) AND DIRECTIVITIES (dB ABOVE ISOTROPIC) FOR LOG-PERIODIC DIPOLE ARRAYS

| $\alpha$ | $\tau = 0.81$ | | $\tau = 0.89$ | | $\tau = 0.95$ | |
|---|---|---|---|---|---|---|
| | $R_{in}$(ohms) | $D_0$(dB) | $R_{in}$(ohms) | $D_0$(dB) | $R_{in}$(ohms) | $D_0$(dB) |
| 10 | 98 | — | 82 | 9.8 | 77.5 | 10.7 |
| 12.5 | — | — | 77 | — | — | — |
| 15 | — | 7.2 | — | — | — | — |
| 17.5 | — | — | 76 | 7.7 | 62 | 8.8 |
| 20 | — | — | 74 | — | — | — |
| 25 | — | — | 63 | 7.2 | — | 8.0 |
| 30 | 80 | — | 64 | — | 54 | — |
| 35 | — | — | 56 | 6.5 | — | — |
| 45 | 65 | 5.2 | 59 | 6.2 | — | — |

SOURCE: D. E. Isbell, "Log Periodic Dipole Arrays," *IRE Trans. Antennas Propagat.*, Vol. AP-8, pp. 260–267, May 1960. © (1960) IEEE.

as defined by (11-25) and (11-26).* Taking the logarithm of both sides in (11-25) reduces to

$$\Delta = \ln(f_2) - \ln(f_1) = \ln\left(\frac{1}{\tau}\right) \tag{11-27}$$

The variations that occur within a given cycle ($f_1 \leq f \leq f_2 = f_1/\tau$) will repeat identically at other cycles of the bandwidth defined by $f_1/\tau^{n-1} \leq f \leq f_1/\tau^n$, $n = 1, 2, 3, \ldots$.

Typical designs of log-periodic dipole arrays have apex half angles of $10° \leq \alpha \leq 45°$ and $0.95 \geq \tau \geq 0.7$. There is a relation between the values of $\alpha$ and $\tau$. As $\alpha$ increases, the corresponding $\tau$ values decrease, and vice versa. Larger values of $\alpha$ or smaller values of $\tau$ result in more compact designs which require smaller number of elements separated by larger distances. In contrast, smaller values of $\alpha$ or larger values of $\tau$ require a larger number of elements that are closer together. For this type of a design, there are more elements in the active region which are nearly $\lambda/2$. Therefore the variations of the impedance and other characteristics as a function of frequency are smaller, because of the smoother transition between the elements, and the gains are larger.

Experimental models of log-periodic dipole arrays have been built and measurements were made [5]. The input impedances (purely resistive) and corresponding directivities (*above isotropic*) for three different designs are listed in Table 11.1. Larger directivities can be achieved by arraying multiple log-periodic dipole arrays. There are other configurations of log-periodic dipole array designs, including those with V instead of linear elements [11]. This array provides moderate bandwidths with good directivities at the higher frequencies, and it is widely used as a single TV antenna covering the entire frequency spectrum from the lowest VHF channel (54 MHz) to the highest UHF (806 MHz). Typical gain, VSWR, and $E$- and $H$-plane half-

*In some cases, the impedance (but not the pattern) may vary with a period which is one-half of (11-27). That is, $\Delta = \frac{1}{2}\ln(1/\tau)$.

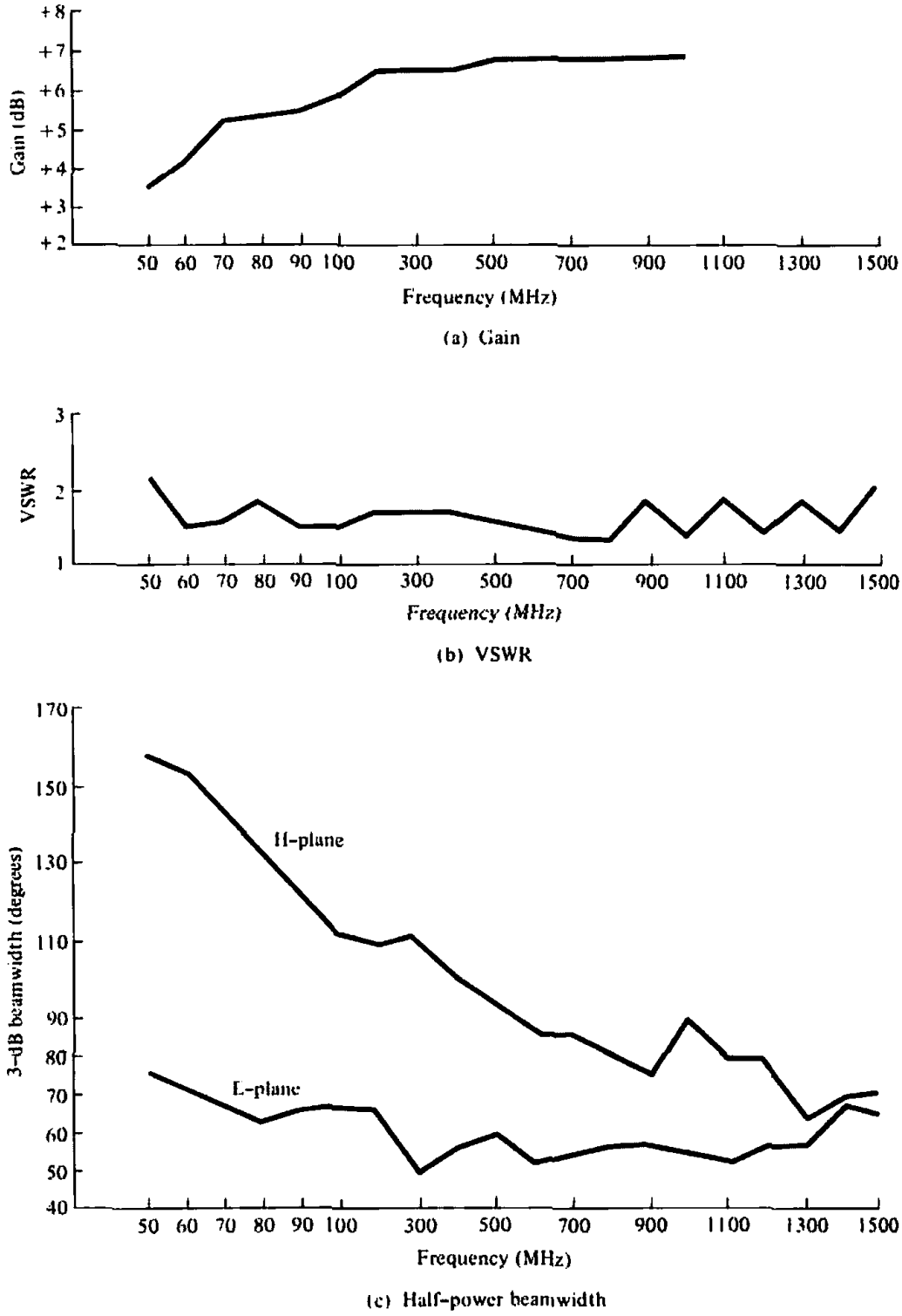


**Figure 11.12** Typical gain, VSWR, and half-power beamwidth of commercial log-periodic dipole arrays. (SOURCE: *Antennas, Antenna Masts and Mounting Adaptors*, American Electronic Laboratories, Inc., Lansdale, Pa., Catalog 7.5M-7-79. Courtesy of American Electronic Laboratories, Inc., Montgomeryville, PA 18936 USA)

power beamwidths of commercial log-periodic dipole arrays are shown in Figures 11.12(a), (b), (c), respectively [8]. The overall length of each of these antennas is about 105 in. (266.70 cm) while the largest element in each has an overall length of about 122 in. (309.88 cm). The weight of each antenna is about 31 lb ($\simeq$14 kg).

### 11.4.3 Design of Dipole Array

The ultimate goal of any antenna configuration is the design that meets certain specifications. Probably the most introductory, complete, and practical design procedure for a log-periodic dipole array is that by Carrel [10]. To aid in the design, he has a set of curves and nomographs. The general configuration of a log-periodic array is described in terms of the design parameters $\tau$, $\alpha$, and $\sigma$ related by

$$\alpha = \tan^{-1}\left[\frac{1-\tau}{4\sigma}\right] \tag{11-28}$$

Once two of them are specified, the other can be found. Directivity (in dB) contour curves as a function of $\tau$ for various values of $\sigma$ are shown in Figure 11.13.

The original directivity contour curves in [10] are in error because the expression for the *E*-plane field pattern in [10] is in error. To correct the error, the leading $\sin(\theta)$ function in front of the summation sign of equation 47 in [10] should be in the denominator and not in the numerator [i.e., replace $\sin\theta$ by $1/\sin(\theta)$] [12]. The influence of this error in the contours of Figure 11.13 is variable and leads to 1–2 dB higher directivities. However it has been suggested that, as an average, the directivity of each original contour curve be reduced by about 1 dB. This has been implemented already, and the curves in Figure 11.13 are more accurate as they now appear.

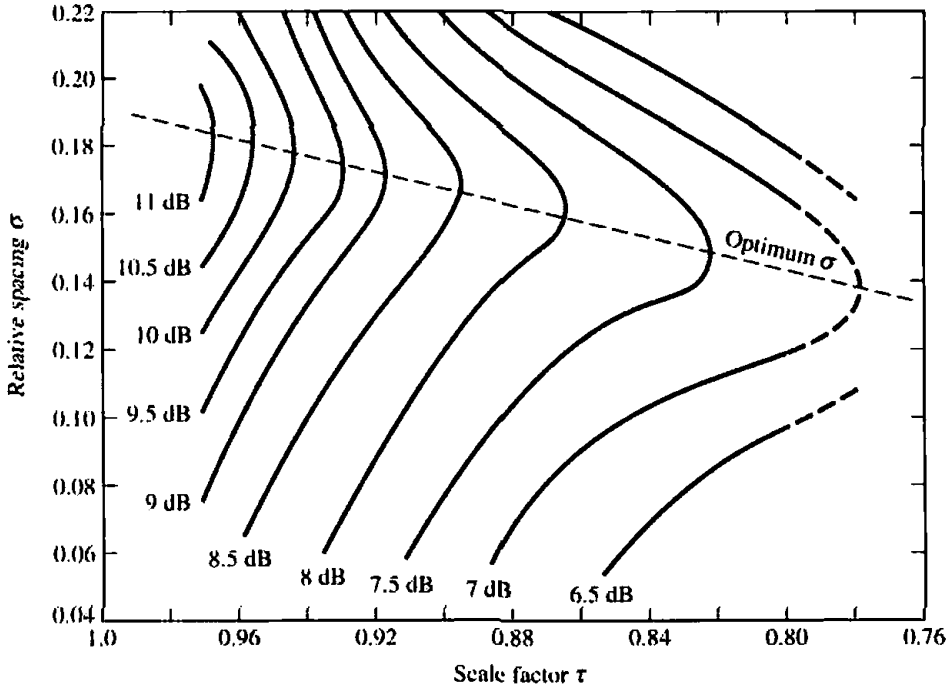


**Figure 11.13** Computed contours of constant directivity versus $\sigma$ and $\tau$ for log periodic dipole arrays. (SOURCE: R. L. Carrel, "Analysis and Design of the Log-Periodic Dipole Antenna," Ph.D. Dissertation, Elec. Eng. Dept., University of Illinois, 1961, University Microfilms, Inc., Ann Arbor Michigan)

*Note:* The initial curves led to designs whose directivities are 1-2 dB too high. They have been reduced by an average of 1dB (see P. C. Butson and G. T. Thompson, "A Note on the Calculation of the Gain of Log-Periodic Dipole Antennas," *IEEE Trans. Antennas Propagat.*, AP-24, pp. 105–106, January 1976).

*A. Design Equations*

In this section a number of equations will be introduced that can be used to design a log-periodic dipole array.

While the bandwidth of the system determines the lengths of the shortest and longest elements of the structure, the width of the active region depends on the specific design. Carrel [10] has introduced a semiempirical equation to calculate the bandwidth of the active region $B_{ar}$ related to $\alpha$ and $\tau$ by

$$B_{ar} = 1.1 + 7.7(1 - \tau)^2 \cot \alpha \tag{11-29}$$

In practice a slightly larger bandwidth ($B_s$) is usually designed than that which is required ($B$). The two are related by

$$B_s = BB_{ar} = B[1.1 + 7.7(1 - \tau)^2 \cot \alpha] \tag{11-30}$$

where

$B_s$ = designed bandwidth
$B$ = desired bandwidth
$B_{ar}$ = active region bandwidth

The total length of the structure $L$, from the shortest ($l_{min}$) to the longest ($l_{max}$) element, is given by

$$L = \frac{\lambda_{max}}{4}\left(1 - \frac{1}{B_s}\right)\cot \alpha \tag{11-31}$$

where

$$\lambda_{max} = 2l_{max} = \frac{v}{f_{min}} \tag{11-31a}$$

From the geometry of the system, the number of elements are determined by

$$N = 1 + \frac{\ln(B_s)}{\ln(1/\tau)} \tag{11-32}$$

The center-to-center spacing $s$ of the feeder line conductors can be determined by specifying the required input impedance (assumed to be real), and the diameter of the dipole elements and the feeder line conductors. To accomplish this, we first define an average characteristic impedance of the elements given by

$$Z_a = 120\left[\ln\left(\frac{l_n}{d_n}\right) - 2.25\right] \tag{11-33}$$

where $l_n/d_n$ is the length-to-diameter ratio of the $n$th element of the array. For an ideal log-periodic design, this ratio should be the same for all the elements of the array. Practically, however, the elements are usually divided into one, two, three or more groups with all the elements in each group having the same diameter but not the same length. The number of groups is determined by the total number of elements of the array. Usually three groups (for the small, middle, and large elements) should be sufficient.

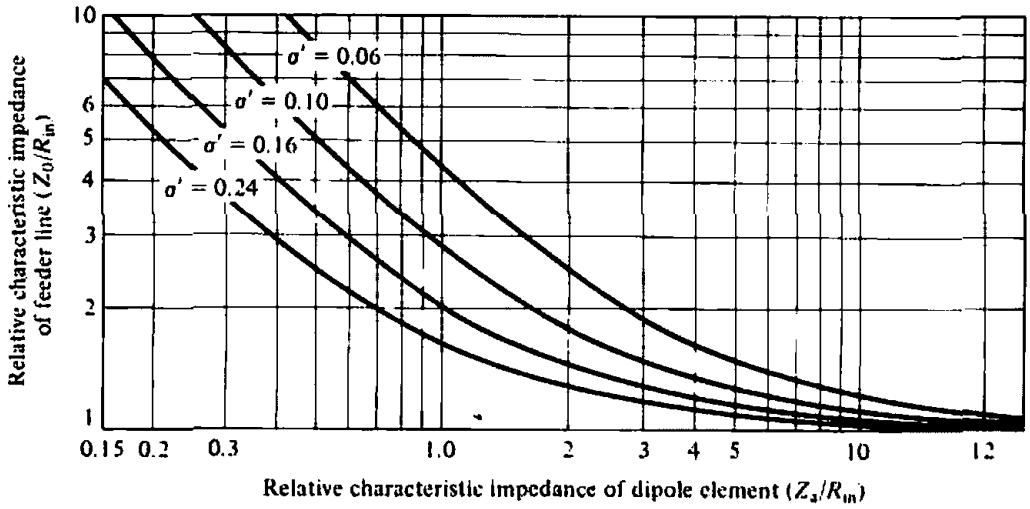


**Figure 11.14** Relative characteristic impedance of a feeder line as a function of relative characteristic impedance of dipole element. (SOURCE: R. L. Carrel, "Analysis and Design of the Log-Periodic Dipole Antenna," Ph.D. Dissertation, Elec. Eng. Dept., University of Illinois, 1961, University Microfilms, Inc., Ann Arbor, Michigan)

The effective loading of the dipole elements on the input line is characterized by the graphs shown in Figure 11.14 where

$\sigma' = \sigma/\sqrt{\tau}$ = relative mean spacing

$Z_a$ = average characteristic impedance of the elements

$R_{in}$ = input impedance (real)

$Z_0$ = characteristic impedance of the feeder line

The center-to-center spacing $s$ between the two rods of the feeder line, each of identical diameter $d$, is determined by

$$s = d \cosh\left(\frac{Z_0}{120}\right) \tag{11-34}$$

*B. Design Procedure*

A design procedure is outlined here, based on the equations introduced above and in the previous page, and assumes that the directivity (in dB), input impedance $R_{in}$ (real), diameter of elements of feeder line ($d$), and the lower and upper frequencies ($B = f_{max}/f_{min}$) of the bandwidth are specified. It then proceeds as follows:

1. Given $D_0$ (dB), determine $\sigma$ and $\tau$ from Figure 11.13.
2. Determine $\alpha$ using (11-28).
3. Determine $B_{ar}$ using (11-29) and $B_s$ using (11-30).
4. Find $L$ using (11-31) and $N$ using (11-32).
5. Determine $Z_a$ using (11-33) and $\sigma' = \sigma/\sqrt{\tau}$.
6. Determine $Z_0/R_{in}$ using Figure 11.14.
7. Find $s$ using (11-34).

**Example 11.1**

Design a log-periodic dipole antenna, of the form shown in Figure 11.9(d), to cover all the VHF TV channels (starting with 54 MHz for channel 2 and ending with 216 MHz for channel 13. See Appendix IX.) The desired directivity is 8 dB and the input impedance is 50 ohms (ideal for a match to 50-ohm coaxial cable). The elements should be made of aluminum tubing with $\frac{3}{4}$ in. (1.9 cm) outside diameter for the largest element and the feeder line and $\frac{3}{16}$ in. (0.48 cm) for the smallest element. These diameters yield identical *l/d* ratios for the smallest and largest elements.

SOLUTION

1. From Figure 11.13, for $D_0 = 8$ dB the optimum $\sigma$ is $\sigma = 0.157$ and the corresponding $\tau$ is $\tau = 0.865$.
2. Using (11-28)

$$\alpha = \tan^{-1}\left[\frac{1 - 0.865}{4(0.157)}\right] = 12.13^\circ \simeq 12^\circ$$

3. Using (11-29)

$$B_{ar} = 1.1 + 7.7(1 - 0.865)^2 \cot(12.13^\circ) = 1.753$$

and from (11-30)

$$B_s = BB_{ar} = \frac{216}{54}(1.753) = 4(1.753) = 7.01$$

4. Using (11-31a)

$$\lambda_{max} = \frac{v}{f_{min}} = \frac{3 \times 10^8}{54 \times 10^6} = 5.556 \text{ m } (18.227 \text{ ft})$$

From (11-31)

$$L = \frac{5.556}{4}\left(1 - \frac{1}{7.01}\right)\cot(12.13^\circ) = 5.541 \text{ m } (18.178 \text{ ft})$$

and from (11-32)

$$N = 1 + \frac{\ln(7.01)}{\ln(1/0.865)} = 14.43 \text{ (14 or 15 elements)}$$

5. $$\sigma' = \frac{\sigma}{\sqrt{\tau}} = \frac{0.157}{\sqrt{0.865}} = 0.169$$

At the lowest frequency

$$l_{max} = \frac{\lambda_{max}}{2} = \frac{18.227}{2} = 9.1135 \text{ ft}$$

$$\frac{l_{max}}{d_{max}} = \frac{9.1135(12)}{0.75} = 145.816$$

Using (11-33)

$$Z_a = 120[\ln(145.816) - 2.25] \simeq 327.88 \text{ ohms}$$

Thus

$$\frac{Z_a}{R_{in}} = \frac{327.88}{50} = 6.558$$

6. From Figure 11.14

$$Z_0 \simeq 1.2R_{in} = 1.2(50) = 60 \text{ ohms}$$

7. Using (11-34), assuming the feeder line conductor is made of the same size tubing as the largest element of the array, the center-to-center spacing of the feeder conductors is

$$s = \frac{3}{4}\cosh\left(\frac{60}{120}\right) = 0.846 \simeq 0.85 \text{ in.}$$

which allows for a 0.1-in. separation between their conducting surfaces.

---

For such a high-gain antenna, this is obviously a good practical design. If a lower gain is specified and designed for, a smaller length will result.

*C. Design and Analysis Computer Program*

A computer program entitled LOG-PERIODIC DIPOLE ARRAY has been developed based on the design equations of (11-28)–(11-34), and Figures 11.13 and 11.14, to design a log-periodic dipole array whose geometry is shown in Figure 11.9(a). Although most of the program is based on the same design equations as outlined in the design subsection, this program takes into account more design specifications than those included in the previous design procedure, and it is more elaborate. Once the design is completed, the computer program can be used to analyze the design of the antenna. It is included at the end of this chapter, and the listing is found in the computer disc available with this book. The program has been developed based on input specifications, which are listed in the program at the end of the chapter. It can be used as a design tool to determine the geometry of the array (including the number of elements and their corresponding lengths, diameters, and positions) along with the radiation characteristics of the array (including input impedance, VSWR, directivity, front-to-back ratio, $E$- and $H$-plane patterns, etc.) based on desired specifications. The input data includes the desired directivity, lower and upper frequency of the operating band, length-to-diameter ratio of the elements, characteristic impedance of the input transmission line, desired input impedance, termination (load) impedance, etc. These and others are listed in the program at the end of the chapter.

The program assumes that the current distribution on each antenna element is sinusoidal. This approximation would be very accurate if the elements were very far from each other. However, in the active region the elements are usually separated by a distance of about $0.1\lambda$ when $\alpha = 15°$ and $\tau = 0.9$. Referring to Figure 8.21, one can see that two $\lambda/2$ dipoles separated by $0.1\lambda$ have a mutual impedance (almost real) of about 70 ohms. If this mutual impedance is high compared to the resistance of the transmission line (not the characteristic impedance), then the primary method of coupling energy to each antenna will be through the transmission line. If the mutual impedance is high compared to the self-impedance of each element, then the effect on the radiation pattern should be small. In practice, this is usually the case, and the approximation is relatively good. However, an integral equation formulation with a

Moment Method numerical solution would be more accurate. The program uses (8-60a) for the self-resistance and (8-60b) for the self-reactance. It uses (8-68) for the mutual impedance, which for the side-by-side configuration reduces to the sine and cosine integrals in [13], similar in form to (8-71a)–(8-71e) for the $l = \lambda/2$ dipole.

The geometry of the designed log-periodic dipole array is that of Figure 11.9, except that the program also allows for an input transmission line (connected to the first/shortest element), a termination transmission line (extending beyond the last/longest element), and a termination (load) impedance. The length of the input transmission line changes the phase of computed data (such as voltage, current, reflection coefficient, etc.) while its characteristic impedance is used to calculate the VSWR, which in turn affects the input impedance measured at the source. The voltages and currents are found based on the admittance method of Kyle [14]. The termination transmission line and the termination (load) impedance allow for the insertion of a matching section whose primary purpose is to absorb any energy which manages to continue past the active region. Without the termination (load) impedance, this energy would be reflected along the transmission line back into the active region where it would affect the radiation characteristics of the array design and performance.

In designing the array, the user has the choice to select $\sigma$ and $\tau$ (but not the directivity) or to select the directivity (but not $\sigma$ and $\tau$). In the latter case, the program finds $\sigma$ and $\tau$ by assuming an *optimum design* as defined by the dashed line of Figure 11.13. For the geometry of the array, the program assumes that the elements are placed along the $z$-axis (with the shortest at $z = 0$ and the longest along the positive $z$-axis). Each linear element of the array is directed along the $y$-axis (i.e., the array lies on the $yz$-plane). The angle $\theta$ is measured from the $z$ axis toward the $xy$-plane while angle $\phi$ is measured from the $x$-axis (which is normal to the plane of the array) toward the $y$-axis along the $xy$-plane. The $E$-plane of the array is the $yz$-plane ($\phi = 90°, 270°$; $0° \leq \theta \leq 180°$) while the $H$-plane is the $xz$-plane ($\phi = 0°, 180°$; $0° \leq \theta \leq 180°$).

## 11.5 FUNDAMENTAL LIMITS OF ELECTRICALLY SMALL ANTENNAS

In all areas of electrical engineering, especially in electronic devices and computers, the attention has been shifted toward miniaturization. Electromagnetics, and antennas in particular, are of no exception. A large emphasis in the last few years has been placed toward electrically small antennas, including printed board designs. However, there are fundamental limits as to how small the antenna elements can be made. The basic limitations are imposed by the free-space wavelength to which the antenna element must couple to, which has not been or is expected to be miniaturized [15].

An excellent paper on the fundamental limits in antennas has been published [15], and most of the material in this section is drawn from it. It reviews the limits of electrically small, superdirective, super-resolution, and high-gain antennas. The limits on electrically small antennas are derived by assuming that the entire antenna structure (with a largest linear dimension of $2r$), and its transmission line and oscillator are all enclosed within a sphere of radius $r$ as shown in Figure 11.15(a). Because of the arbitrary current or source distribution of the antenna inside the sphere, its radiated field outside the sphere is expressed as a complete set of orthogonal spherical vector waves or modes. For vertically polarized omnidirectional antennas, only $TM_{m0}$ circularly symmetric (no azimuthal variations) modes are required. Each mode is used to represent a spherical wave which propagates in the outward radial direction. This approach was introduced first by Chu [16], and it was followed by Harrington [17].

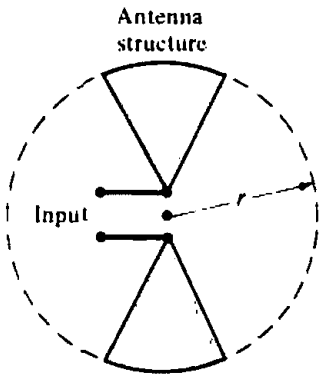


(a) Biconical antenna within a sphere (after C. J. Chu [13])

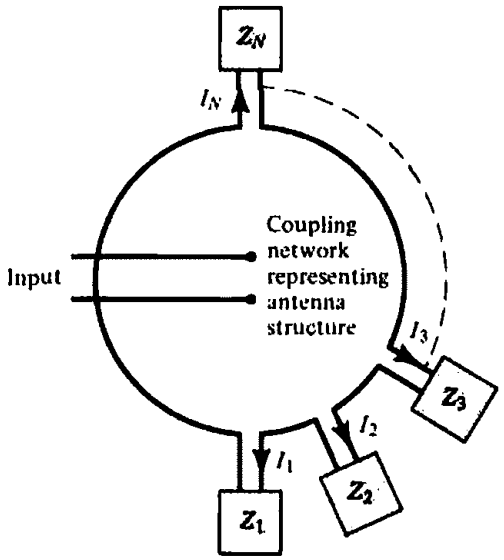


(b) Equivalent network of a vertically-polarized omnidirectional antenna (after C. J. Chu [13])

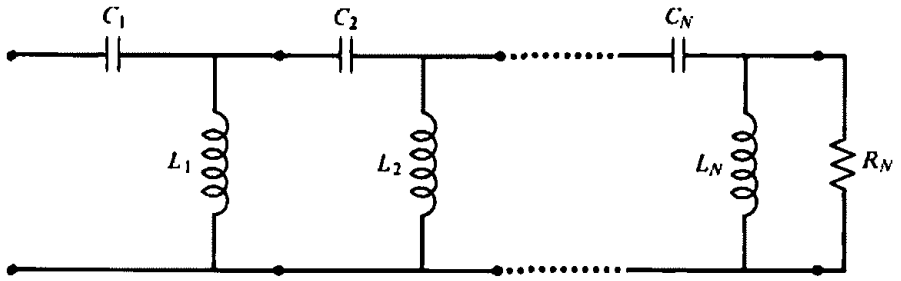


(c) Equivalent circuit for $N$ spherical modes

**Figure 11.15** Antenna within a sphere of radius $r$, and its equivalent circuit modeling. (SOURCE: C. J. Chu, "Physical Limitations of Omnidirectional Antennas," *J. Appl. Phys.*, Vol. 19, pp. 1163–1175, December 1948)

Earlier papers on the fundamental limitations and performance of small antennas were published by Wheeler [18]–[20]. He derived the limits of a small dipole and a small loop (used as a magnetic dipole) from the limitations of a capacitor and an inductor, respectively. The capacitor and inductor were chosen to occupy, respectively, volumes equal to those of the dipole and the loop.

Using the mathematical formulation introduced by Chu [16], the source or current distribution of the antenna system inside the sphere is not uniquely determined by the field distribution outside the sphere. Since it is possible to determine an infinite number of different source or current distributions inside the sphere, for a given field configuration outside the sphere, Chu [16] confined his interest to the most favorable source distribution and its corresponding antenna structure that could exist within the sphere. This approach was taken to minimize the details and to simplify the task of identifying the antenna structure. It was also assumed that the desired current or source distribution minimizes the amount of energy stored inside the sphere so that the input impedance at a given frequency is resistive.

Because the spherical wave modes outside the sphere are orthogonal, the total energy (electric or magnetic) outside the sphere and the complex power transmitted across the closed spherical surface are equal, respectively, to the sum of the energies

and complex powers associated with each corresponding spherical mode. Therefore there is no coupling, in energy or power, between any two modes outside the sphere. As a result, the space outside the sphere can be replaced by a number of independent equivalent circuits as shown in Figure 11.15(b). The number of equivalent circuits is equal to the number of spherical wave modes outside the sphere, plus one. The terminals of each equivalent circuit are connected to a box which represents the inside of the sphere, and from inside the box a pair of terminals are drawn to represent the input terminals. Using this procedure, the antenna space problem has been reduced to one of equivalent circuits.

The radiated power of the antenna is calculated from the propagating modes while all modes contribute to the reactive power. When the sphere (which encloses the antenna element) becomes very small, there exist no propagating modes. Therefore the $Q$ of the system becomes very large since all modes are evanescent (below cutoff) and contribute very little power. However, unlike closed waveguides, each evanescent mode here has a real part (even though it is very small).

For a lossless antenna (radiation efficiency $e_{cd} = 100\%$), the equivalent circuit of each spherical mode is a single network section with a series $C$ and a shunt $L$. The total circuit is a ladder network of $L - C$ sections (one for each mode) with a final shunt resistive load, as shown in Figure 11.15(c). The resistive load is used to represent the normalized antenna radiation resistance.

From this circuit structure, the input impedance is found. The $Q$ of each mode is formed by the ratio of its stored to its radiated energy. When several modes are supported, the $Q$ is formed from the contributions of all the modes.

It has been shown that the higher order modes within a sphere of radius $r$ become evanescent when $kr < 1$. Therefore the $Q$ of the system, for the lowest order TM mode, reduces to [15]

$$Q = \frac{1 + 2(kr)^2}{(kr)^3[1 + (kr)^2]} \overset{kr \ll 1}{\simeq} \frac{1}{(kr)^3} \tag{11-35}$$

When two modes are excited, one TE and the other TM, the values of $Q$ are halved. Equation (11-35), which relates the lowest achievable $Q$ to the largest linear dimension of an electrically small antenna, is independent of the geometrical configuration of the antenna within the sphere of radius $r$. The shape of the radiating element within the bounds of the sphere only determines whether TE, TM, or TE and TM modes are excited. *Therefore (11-35) represents the fundamental limit on the electrical size of an antenna.* In practice, this limit is only approached but is never exceeded or even equaled.

The losses of an antenna can be taken into account by including a loss resistance in series with the radiation resistance, as shown by the equivalent circuits of Figures 2.21(b) and 2.22(b). This influences the $Q$ of the system and the antenna radiation efficiency as given by (2-90).

Computed values of $Q$ versus $kr$ for idealized antennas enclosed within a sphere of radius $r$, and with radiation efficiences of $e_{cd} = 100$, 50, 10, and 5, are shown plotted in Figure 11.16. These curves represent the minimum values of $Q$ that can be obtained from an antenna whose structure can be enclosed within a sphere of radius $r$ and whose radiated field, outside the sphere, can be represented by a single spherical wave mode.

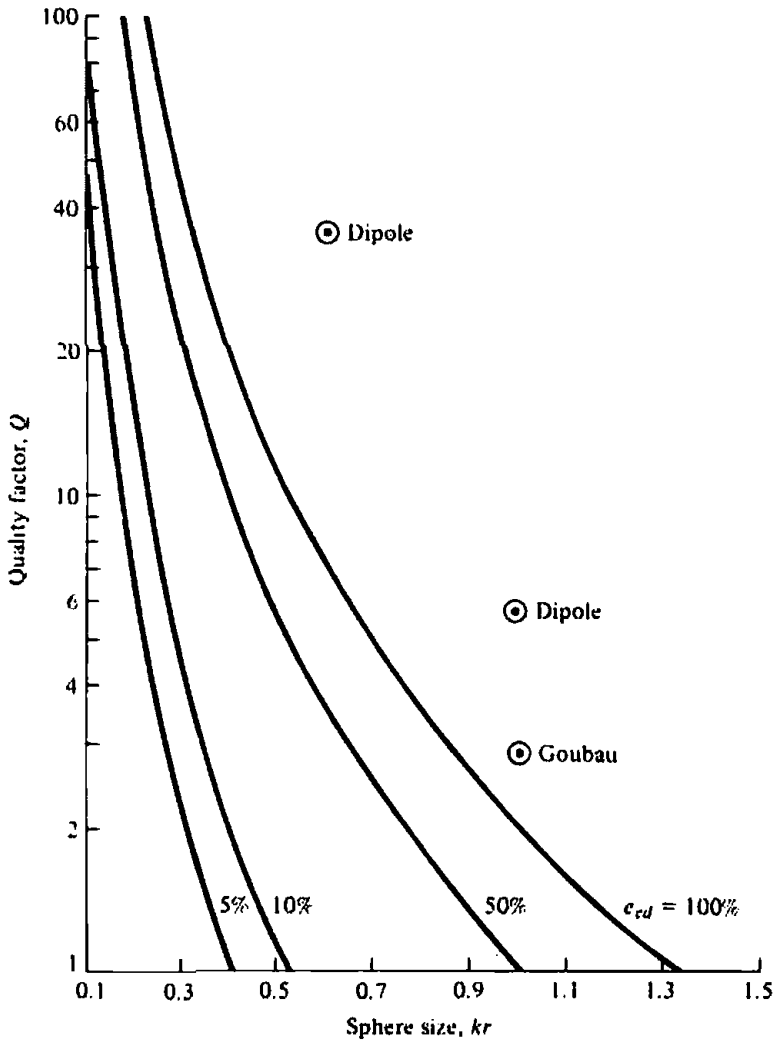


**Figure 11.16** Fundamental limits of $Q$ versus antenna size (enclosed within a sphere of radius $r$) for single-mode antennas of various radiation efficiencies. (SOURCE: R. C. Hansen, "Fundamental Limitations in Antennas," *Proc. IEEE*, Vol. 69, No. 2, February 1981. © (1981) IEEE)

For antennas with equivalent circuits of fixed values, the fractional bandwidth is related to the $Q$ of the system by

$$\text{fractional bandwidth} = \text{FBW} = \frac{\Delta f}{f_0} = \frac{1}{Q} \tag{11-36}$$

where

$f_0$ = center frequency
$\Delta f$ = bandwidth

The relationship of (11-36) is valid for $Q \gg 1$ since the equivalent resonant circuit with fixed values is a good approximation for an antenna. For values of $Q < 2$, (11-36) is not accurate.

To compare the results of the minimum $Q$ curves of Figure 11.16 with values of practical antenna structures, data points for a small linear dipole and a Goubau [21]

antenna are included in the same figure. For a small linear dipole of length $l$ and wire radius $a$, its impedance is given by [15]

$$Z_{in} \simeq 20\pi^2\left(\frac{l}{\lambda}\right)^2 - j120\frac{\left[\ln\left(\frac{l}{2a}\right) - 1\right]}{\tan\left(\pi\frac{l}{\lambda}\right)} \tag{11-37}$$

and its corresponding $Q$ by

$$Q \simeq \frac{\left[\ln\left(\frac{l}{2a}\right) - 1\right]}{\left(\pi\frac{l}{\lambda}\right)^2 \tan\left(\pi\frac{l}{\lambda}\right)} \tag{11-38}$$

The real part in (11-37) is identical to (4-37). The computed $Q$ values of the small dipole were for $kl/2 = kr \simeq 0.62$ and 1.04 with $l/2a = l/d = 50$, and of the Goubau antenna were for $kr \simeq 1.04$.

It is apparent that the $Q$'s of the dipole are much higher than the corresponding values of the minimum $Q$ curves even for the 100% efficient antennas. However the Goubau antenna, of the same radius sphere, demonstrates a lower value of $Q$ and approaches the values of the 100% minimum $Q$ curve. This indicates that the fractional bandwidth of the Goubau antenna, which is inversely proportional to its $Q$ as defined by (11-36), is higher than that of a dipole enclosed within the same radius sphere. In turn, the bandwidth of an idealized antenna, enclosed within the same sphere, is even larger.

From the above, it is concluded that *the bandwidth of an antenna (which can be closed within a sphere of radius r) can be improved only if the antenna utilizes efficiently, with its geometrical configuration, the available volume within the sphere.* The dipole, being a one-dimensional structure, is a poor utilizer of the available volume within the sphere. However a Goubau antenna, being a clover leaf dipole with coupling loops over a ground plane (or a double cover leaf dipole without a ground plane), is a more effective design for utilizing the available three-dimensional space within the sphere. A design that utilizes the space even more efficiently than the Goubau antenna would possess a lower $Q$ and a higher fractional bandwidth. Ultimately, the values would approach the minimum $Q$ curves. In practice, these curves are only approached but are never exceeded or even equaled.

## References


1. V. H. Rumsey, "Frequency Independent Antennas," *1957 IRE National Convention Record*, pt. 1, pp. 114–118.
2. J. D. Dyson, "The Equiangular Spiral Antenna," *IRE Trans. Antennas Propagat.*, Vol. AP-7, pp. 181–187, April 1959.
3. J. D. Dyson, "The Unidirectional Equiangular Spiral Antenna," *IRE Trans. Antennas Propagat.*, Vol. AP-7, pp. 329–334, October 1959.
4. R. H. DuHamel and D. E. Isbell, "Broadband Logarithmically Periodic Antenna Structures," *1957 IRE National Convention Record*, pt. 1, pp. 119–128.
5. D. E. Isbell, "Log Periodic Dipole Arrays," *IRE Trans. Antennas Propagat.*, Vol. AP-8, pp. 260–267, May 1960.

6. R. S. Elliott, "A View of Frequency Independent Antennas," *The Microwave Journal*, pp. 61–68, December 1962.
7. H. G. Booker, "Slot Aerials and Their Relation to Complementary Wire Aerials," *Journal of IEE* (London), Vol. 93, pt. IIIA, April 1946.
8. *Antennas, Antenna Masts and Mounting Adaptors*, American Electronic Laboratories, Inc., Lansdale, PA, Catalog 7.5M-7-79.
9. R. H. DuHamel and F. R. Ore, "Logarithmically Periodic Antenna Designs," *IRE National Convention Record*, pt. 1, pp. 139–152, 1958.
10. R. L. Carrel, "Analysis and Design of the Log-Periodic Dipole Antenna," Ph.D. Dissertation, Elec. Eng. Dept., University of Illinois, 1961, University Microfilms, Inc., Ann Arbor, MI.
11. P. E. Mayes and R. L. Carrel, "Log-Periodic Resonant-V Arrays," presented at WESCON, San Francisco, California, August 22–25, 1961.
12. P. C. Budson and G. T. Thompson, "A Note on the Calculation of the Gain of Log-Periodic Dipole Antennas," *IEEE Trans. Antennas Propagat.*, AP-24, pp. 105–106, January 1976.
13. H. E. King, "Mutual Impedance of Unequal Length Antennas in Echelon," *IRE Trans. Antennas Propagat.*, Vol. AP-5, pp. 306–313, July 1957.
14. R. H. Kyle, "Mutual Coupling Between Log-Periodic Dipole Antennas," General Electric Tech. Info. Series, Report No. R69ELS-3, December 1968.
15. R. C. Hansen, "Fundamental Limitations in Antennas," *Proc. IEEE*, Vol. 69, No. 2, February 1981.
16. L. J. Chu, "Physical Limitations of Omnidirectional Antennas," *J. Appl. Phys.*, Vol. 19, pp. 1163–1175, December 1948.
17. R. F. Harrington, "Effect of Antenna Size on Gain, Bandwidth, and Efficiency," *J. Res. Nat. Bur. Stand.-D, Radio Propagation*, Vol. 64D, pp. 1–12, January–February 1960.
18. H. A. Wheeler, "Fundamental Limitations of Small Antennas," *Proc. IRE*, pp. 1479–1488, December 1947.
19. H. A. Wheeler, "The Radiansphere Around a Small Antenna," *Proc. IRE*, pp. 1325–1331, August 1959.
20. H. A. Wheeler, "Small Antennas," *IEEE Trans. Antennas Propagat.*, Vol. AP-23, No. 4, pp. 462–469, July 1975.
21. G. Goubau, "Multi-element Monopole Antennas," *Proc. Workshop on Electrically Small Antennas ECOM*, Ft. Monmouth, N. J., pp. 63–67, May 1976.

## *PROBLEMS*

11.1. Design a symmetrical two-wire plane spiral ($\phi_0 = 0, \pi$) at $f = 10$ MHz with total feed terminal separation of 10 $^{3}\lambda$. The total length of each spiral should be one wavelength and each wire should be of one turn.
   (a) Determine the rate of spiral of each wire.
   (b) Find the radius (in $\lambda$ and in meters) of each spiral at its terminal point.
   (c) Plot the geometric shape of one wire. Use meters for its length.

11.2. Verify (11-28).

11.3. Design log-periodic dipole arrays, of the form shown in Figure 11.9(d), each with directivities of 9 dB, input impedance of 75 ohms, and each with the following additional specifications: Cover the (see Appendix IX)
   (a) VHF TV channels 2–13 (54–216 MHz). Use aluminum tubing with outside diameters of $\frac{3}{4}$ in. (1.905 cm) and $\frac{3}{16}$ in. (0.476 cm) for the largest and smallest elements, respectively.
   (b) VHF TV channels 2–6 (54–88 MHz). Use diameters of 1.905 and 1.1169 cm for the largest and smallest elements, respectively.
   (c) VHF TV channels 7–13 (174–216 MHz). Use diameters of 0.6 and 0.476 cm for the largest and smallest elements, respectively.

(d) UHF TV channels (512–806 MHz). The largest and smallest elements should have diameters of 0.2 and 0.128 cm, respectively.
(e) FM band of 88–108 MHz (100 channels at 200 KHz apart). The largest and smallest elements should have diameters of 1.169 and 0.9525 cm, respectively.

In each design, the feeder line should have the same diameter as the largest element.

11.4. For each design in Problem 11.3, determine the
(a) span of each period over which the radiation characteristics will vary slightly
(b) number of periods (cycles) within the desired bandwidth

11.5. Using the LOG-PERIODIC DIPOLE ARRAY computer program and Appendix IX, design an array which covers the VHF television band. Design the antenna for 7 dBi gain optimized in terms of $\sigma$-$\tau$. The antenna should be matched to a 75-ohm coaxial input cable. For this problem, set the input line length to 0 meters, the source resistance to 0 ohms, the termination line length to 0 meters, the termination impedance to 100 Kohms, the length-to-diameter ratio to 40, and the boom diameter to 10 cm. To make the actual input impedance 75 ohms, one must iteratively find the optimal desired input impedance.
(a) Plot the gain, magnitude of the input impedance, and VSWR versus frequency from 30 MHz to 400 MHz.
(b) Based on the ripples in the plot of gain versus frequency, what is $\tau$? Compare this value to the value calculated by the computer program.
(c) Why does the gain decrease rapidly for frequencies less than the lower design frequency yet decrease very slowly for frequencies higher than the upper design frequency?

11.6. For the antenna of Problem 11.5, replace the 100-Kohm load with a 75-ohm resistor.
(a) Plot the gain, magnitude of the input impedance, and VSWR versus frequency from 30 MHz to 400 MHz.
(b) What does the termination resistor do which makes this antenna an improvement over the antenna of Problem 11.5?

11.7. For the antenna of Problem 11.5, replace the 100-Kohm termination (load) with a 75-ohm resistor and make the source resistance 10 ohms. This resistance represents the internal resistance of the power supply as well as losses in the input line.
(a) Plot the gain versus frequency from 30 MHz to 400 MHz.
(b) What is the antenna efficiency of this antenna?
(c) Based on your result from parts (a) and (b), what should the gain versus frequency plot look like for Problem 11.6?

11.8. Design a log-periodic dipole array which operates from 470 MHz to 806 MHz (UHF band) with 8 dBi gain. This antenna should be matched to a 50-ohm cable of length 2 meters with no source resistance. The termination should be left open. Select the length-to-diameter ratio to be 25. At 600 MHz, do the following. Use the computer program at the end of this chapter.
(a) Plot the E- and H- plane patterns.
(b) Calculate the E- and H-plane half-power beamwidths.
(c) Find the front-to-back ratio.
(d) Why does the E-plane pattern have deep nulls while the H-plane pattern does not?

11.9. The overall length of a small linear dipole antenna (like a biconical antenna, or cylindrical dipole, or any other) is $\lambda/\pi$. Assuming the antenna is 100% efficient, what is:
(a) The smallest possible value of $Q$ for an antenna of such a length? Practically it will be larger than that value.
(b) The largest fractional bandwidth ($\Delta f/f_0$ where $f_0$ is the center frequency)

11.10. It is desired to design a 100% efficient biconical dipole antenna whose overall length is $\lambda/20$. The design guidelines specify a need to optimize the frequency response (bandwidth). To accomplish this, the quality factor $Q$ of the antenna should be minimized. In order to get some indications as to the fundamental limits of the design:
(a) What is the lowest possible limit of the $Q$ for this size antenna?
(b) In order to approach this lower fundamental limit, should the included angle of the biconical antenna be made larger or smaller, and why?

## *COMPUTER PROGRAM - LOG-PERIODIC DIPOLE ARRAY*

```
C*****************************************************************
C
C     THIS IS A FORTRAN PROGRAM, AND IT DESIGNS AND ANALYZES A
C     LOG-PERIODIC DIPOLE ARRAY BASED ON THE GEOMETRY OF FIGURE
C     11.9(a), THE DATA IN FIGURES 11.13 AND 11.14, AND THE DESIGN
C     EQUATIONS OF (11-28) - (11-34).
C
C     THE USER CAN TAILOR THE DESIGN AND ANALYSIS BY FOLLOWING
C     THE LISTED STEPS AND SELECTING THE APPROPRIATE OPTIONS.
C     FOR MORE DETAILS, SEE THE LPDA.DOC FILE IN THE COMPUTER DISC.
C
C     **DESIGN PROCEDURE
C
C        STEP I: CHOOSE ONE OF THE FOLLOWING OPTIONS
C          · SPECIFY σ AND τ. THIS SETS THE DIRECTIVITY.
C          · SPECIFY THE DIRECTIVITY. THIS SETS σ AND τ FOR
C            OPTIMUM DIRECTIVITY DESIGN.
C        STEP II: CHOOSE ONE OF THE FOLLOWING OPTIONS
C          · CHOOSE THE BOOM SPACING AND BOOM DIAMETER. THIS
C            SETS THE CHARACTERISTIC IMPEDANCE OF THE
C            TRANSMISSION LINE.
C          · CHOOSE THE DESIRED INPUT IMPEDANCE AND BOOM
C            DIAMETER. THIS SETS THE BOOM SPACING.
C        STEP III: CHOOSE ONE OF THE FOLLOWING OPTIONS
C          · ROUND THE CALCULATED ELEMENT DIAMETERS TO THE
C            NEAREST AVAILABLE WIRE DIAMETERS.
C          · DO NOT ROUND THE CALCULATED ELEMENT DIAMETERS.
C
C     AFTER CHOOSING THE DESIGN OPTIONS, PROCEED TO THE
C     ANALYSIS. THE OUTPUT DEPENDS ON ANALYSIS OPTIONS CHOSEN.
C
C     **ANALYSIS PROCEDURE
C
C        STEP IV: SELECT ANY COMBINATION OF THE FOLLOWING OPTIONS
C                 (DO ONE, TWO, THREE OR ALL OF THE FOLLOWING)
C          · NO ANALYSIS
C            OUTPUT: •DESIGN SUMMARY (lists physical parameters and geometry)
C          · ANALYZE DESIGN AT A SINGLE FREQUENCY
C            OUTPUT: •DESIGN SUMMARY (lists physical parameters and geometry)
C                    •E- AND H-PLANE PATTERN ANALYSIS
C                    •CRITICAL PARAMETERS AT ANALYSIS FREQUENCY
C          · ANALYZE DESIGN AT A SINGLE FREQUENCY
C            OUTPUT: •DESIGN SUMMARY (lists physical parameters and geometry)
C                    •CUSTOM-PLANE PATTERN ANALYSIS
C                    •CRITICAL PARAMETERS AT ANALYSIS FREQUENCY
C          · ANALYZE DESIGN OVER A FREQUENCY BAND
C            OUTPUT: •DESIGN SUMMARY (lists physical parameters and geometry)
C                    •CRITICAL PARAMETERS AS A FUNCTION OF
C                     FREQUENCY, INCLUDING GAIN AT BORESIGHT
C
C                                          (continued on next page)
```

```
C                                                          (continued)
C
C     TO COMPLETE THE DESIGN AND ANALYSIS OF ANY OPTION, THE
C     FOLLOWING INPUT AND OUTPUT PARAMETERS WILL GENERALLY BE
C     EITHER SPECIFIED OR CALCULATED. NOT ALL THE PARAMETERS ARE
C     REQUIRED FOR ALL DESIGN AND DESIGN OPTIONS.
C
C       **INPUT PARAMETERS FOR ARRAY DESIGN
C       1. Title    = NAME OF DESIGN
C       2. DO       = DESIRED DIRECTIVITY (dBi)
C       3. Fhigh    = UPPER DESIGN FREQUENCY (MHz)
C       4. Flow     = LOWER DESIGN FREQUENCY (MHz)
C       5. Rs       = SOURCE RESISTANCE (ohms)
C       6. ZCin     = CHARACTERISTIC IMPEDANCE OF INPUT LINE (ohms)
C       7. Rin      = DESIRED INPUT IMPEDANCE (REAL); TYPICALLY
C                     EQUAL TO CHARACTERISTIC IMPEDANCE ZCin
C       8. LLin     = LENGTH OF THE INPUT TRANSMISSION LINE; FROM
C                     THE SOURCE TO FIRST/SHORTEST ELEMENT (m)
C       9. Zout     = TERMINATION IMPEDANCE (ohms); TYPICALLY EQUAL
C                     TO CHARACTERISTIC IMPEDANCE ZCin
C      10. LLout    = LENGTH OF THE TERMINATION TRANSMISSION LINE;
C                     FROM THE LAST-LONGEST ELEMENT TO THE LOAD (m)
C      11. LD       = DESIRED LENGTH-TO-DIAMETER RATIO OF ELEMENTS
C      12. Navail   = NO. OF AVAILABLE ELEMENT DIAMETERS (dimensionless)
C      13. Davail   = DIAMETERS OF AVAILABLE WIRES OR TUBES (cm)
C      14. SB       = CENTER-TO-CENTER BOOM SPACING (cm)
C      15. DB       = DIAMETER OF BOOM TUBES OR WIRES (cm)
C      16. AFSEH    = ANALYSIS FREQ. FOR E- AND H-PATTERNS (MHz)
C      17. AFSC     = ANALYSIS FREQ. FOR CUSTOM PLANE PATTERN (MHz)
C      18. AFhigh   = HIGHEST FREQ. FOR SWEPT FREQUENCY DATA (MHz)
C      19. AFlow    = LOWEST FREQ. FOR SWEPT FREQUENCY DATA (MHz)
C      20. Phi      = ANGLE OF PLANE [(E-, H-) AND/OR CUSTOM] (degrees)
C
C       **PROGRAM OUTPUT OF ARRAY DESIGN
C       1. N        = NUMBER OF ANTENNA ELEMENTS (integer)
C       2. L        = LENGTHS OF ANTENNA ELEMENTS (m)
C       3. ZL       = STATION (POSITION) OF EACH ARRAY ELEMENT (m)
C       4. D        = DIAMETER OF EACH ARRAY ELEMENT (cm)
C       5. VSWR     = VSWR IN INPUT TRANSMISSION LINE
C       6. ZinA     = ACTUAL INPUT IMPEDANCE OF DESIGN (ohms)
C       7. DOA      = ACTUAL DIRECTIVITY OF DESIGN ALONG (dBi)
C       8. PDO      = PEAK DIRECTIVITY ALONG ANY AXIS (dBi)
C       9. FTBR     = FRONT-TO-BACK RATIO OF AMPLITUDE PATTERN (dB)
C      10. FSLL     = FRONT-TO-MAXIMUM SIDE LOBE LEVEL (dB)
C      11. Iin      = CURRENT IN INPUT TRANSMISSION LINE (A)
C      12. Iel      = CURRENTS IN ARRAY ELEMENTS (A)
C      13. Iout     = CURRENT IN TERMINATION TRANSMISSION LINE (A)
C      14. Vin      = VOLTAGE AT THE SOURCE (V)
C      15. Vel      = VOLTAGES OF ARRAY ELEMENTS (V)
C      16. Vout     = VOLTAGE AT THE LOAD (V)
C      17. Epat     = E-PLANE PATTERN (dBi)
C      18. Hpat     = H-PLANE PATTERN (dBi)
C      19. Cpat     = ANY DESIRED CUSTOM PLANE PATTERN (dBi)
C*************************************************************
```